ATTORNEY DOCKET NO.: 0492611-0454 (MIT 8813)

IN THE UNITED STATES PATENT AND TRADEMARK OFFICE

Applicant:	Kisiday, et al.	Examiner:	D. Naff
Serial No.:	09/778,200	Art Unit:	1651
Filed:	February 6, 2001		
For:	PEPTIDE SCAFFOLD ENCAPSULATION OF TISSUE CELLS AND USES THEREOF		

Commissioner for Patents
PO Box 1450
Alexandria, VA 22313-1450

Sir:

DECLARATION UNDER 37 C.F.R. 1.132

We, John Kisiday, Alan Grodzinsky, and Shuguang Zhang declare as follows:

1. We are the inventors of the subject matter disclosed and claimed in United States patent application Serial No. 09/778,200 ('200 application) filed February 6, 2001, and entitled "PEPTIDE SCAFFOLD ENCAPSULATION OF TISSUE CELLS AND USES THEREOF".

2. This Declaration is presented for the purpose of removing from consideration by the Examiner an abstract by Kisiday et al., entitled "A New Self-Assembling Peptide Gel for Cartilage Tissue Engineering: Chondrocyte Encapsulation and Matrix Production", International Cartilage Repair Society, 3rd Symposium, Gothenberg, Sweden, April 27 - 29, (2000) (Reference "R"). The conference began on April 27, 2000, at which time the above-referenced abstract was available to the public in this country. The present Declaration is presented in accordance with *Ex Parte Magner*, 133 USPQ 404 (CCPA 1961) and *In re Katz*, 215 USPQ 14, 18 (CCPA1982) and establishes that the allegedly anticipatory material in Reference R was not invented by another.

3. John Kisiday, Alan Grodzinsky, and Shuguang Zhang are the inventors on the instant application and are also three of the co-authors of Reference R.

4. Moonsoo Jin, Bodo Kurz, and Han-hwa Hung are co-authors of Reference R. These individuals are not inventors of the claimed invention.

5. John Kisiday, Alan Grodzinsky, and Shuguang Zhang mutually conceived and reduced to practice the invention recited in the claims of the '200 application.

6. To the extent that Reference R discloses the claimed invention, the authors of Reference R derived this subject matter from us, the inventors of the '200 application. The inventors communicated the subject matter of the claimed invention to Moonsoo Jin, Bodo Kurz, and Han-hwa Hung, who provided technical assistance under the inventors' direction. The authors of Reference R are not the inventors of the subject matter of the '945 application.

7. All statements made herein of our own knowledge are true and that all statements made on information and belief are believed to be true; and further that these statements were made with the knowledge that willful, false statements and the like so made are punishable by fine or imprisonment, or both, under Section 1001 of Title 18 of the United States Code and that such willful, false statements may jeopardize the validity of the application or any patents issued thereon.

John Kisiday, Ph.D.

9/25/03

Date

Alan Grodzinsky, Ph.D.

9/22/03

Date

Shuguang Zhang, M.D.

9/22/03

Date

3595448_1.DOC

Entrez PubMed
Overview
Help | FAQ
Tutorial
New/Noteworthy
E-Utilities

PubMed Services
Journals Database
MeSH Database
Single Citation Matcher
Batch Citation Matcher
Clinical Queries
LinkOut
Cubby

Related Resources
Order Documents
NLM Gateway
TOXNET
Consumer Health
Clinical Alerts
ClinicalTrials.gov
PubMed Central

Privacy Policy

1: Cappello P, Caorsi C, Bosticardo M, De Angelis S, Novelli F, Forni G, Giovarelli M. Links

CCL16/LEC powerfully triggers effector and antigen-presenting functions of macrophages and enhances T cell cytotoxicity.
J Leukoc Biol. 2003 Oct 2 [Epub ahead of print]
PMID: 14525962 [PubMed - as supplied by publisher]

2: Fujiyama S, Amano K, Uehira K, Yoshida M, Nishiwaki Y, Nozawa Y, Jin D, Takai S, Miyazaki M, Egashira K, Imada T, Iwasaka T, Matsubara H. Links

Bone Marrow Monocyte Lineage Cells Adhere on Injured Endothelium in a Monocyte Chemoattractant Protein-1-Dependent Manner and Accelerate Reendothelialization as Endothelial Progenitor Cells.
Circ Res. 2003 Oct 2 [Epub ahead of print]
PMID: 14525810 [PubMed - as supplied by publisher]

3: D'Orsogna MR, Suchard MA, Chou T. Links

Interplay of chemotaxis and chemokinesis mechanisms in bacterial dynamics.
Phys Rev E Stat Nonlin Soft Matter Phys. 2003 Aug;68(2-1):021925. Epub 2003 Aug 29.
PMID: 14525024 [PubMed - as supplied by publisher]

4: Kunkel EJ, Butcher EC. Links

Plasma-cell homing.
Nat Rev Immunol. 2003 Oct;3(10):822-9.
PMID: 14523388 [PubMed - in process]

5: Tsuge T, Suzuki Y, Shimokawa T, Horikoshi S, Okumura K, Ra C, Tomino Y. Related Articles, Links

Monocyte chemoattractant protein (MCP)-1 production via functionally reconstituted Fcalpha receptor (CD89) on glomerular mesangial cells.
Inflamm Res. 2003 Oct;52(10):428-32.
PMID: 14520519 [PubMed - in process]

6: Miki K, Miki M, Nakamura Y, Suzuki Y, Okano Y, Ogushi F, Ohtsuki Y, Nakayama T. Related Articles, Links

Early-phase neutrophilia in cigarette smoke-induced acute eosinophilic pneumonia.
Intern Med. 2003 Sep;42(9):839-45.
PMID: 14518673 [PubMed - in process]

7: Amano S, Yamagishi S, Inagaki Y, Okamoto T. Related Articles, Links

Angiotensin II stimulates platelet-derived growth factor-B gene expression in cultured retinal pericytes through intracellular reactive oxygen species generation.
Int J Tissue React. 2003;25(2):51-5.
PMID: 14518593 [PubMed - in process]

8: Hayashidani S, Tsutsui H, Shiomi T, Ikeuchi M, Matsusaka H, Suematsu N, Wen J, Egashira K, Takeshita A. Related Articles, Links

Anti-Monocyte Chemoattractant Protein-1 Gene Therapy Attenuates Left Ventricular Remodeling and Failure After Experimental Myocardial Infarction.
Circulation. 2003 Sep 29 [Epub ahead of print]
PMID: 14517168 [PubMed - as supplied by publisher]

Limits: **Publication Date from 1900/01/01 to 2001/02/06**

1: Asadullah K, Docke WD, Volk HD, Sterry W. Related Articles, Links

The pathophysiological role of cytokines in psoriasis.
Drugs Today (Barc). 1999 Dec;35(12):913-24.
PMID: 12973418 [PubMed - in process]

2: Seagrave JC, Nikula KJ. Related Articles, Links

Multiple modes of responses to air pollution particulate materials in A549 alveolar type II cells.
Inhal Toxicol. 2000;12 Suppl 4:247-60.
PMID: 12881895 [PubMed - indexed for MEDLINE]

3: Ball BR, Smith KR, Veranth JM, Aust AE. Related Articles, Links

Bioavailability of iron from coal fly ash: mechanisms of mobilization and of biological effects.
Inhal Toxicol. 2000;12 Suppl 4:209-25. Review.
PMID: 12881893 [PubMed - indexed for MEDLINE]

4: Moqbel R, Lacy P. Related Articles, Links

Molecular mechanisms in eosinophil activation.
Chem Immunol. 2000;78:189-98. Review. No abstract available.
PMID: 12847730 [PubMed - indexed for MEDLINE]

5: Ying S. Related Articles, Links

C-C chemokine expression in atopic and nonatopic asthma.
Chem Immunol. 2000;78:178-88. Review. No abstract available.
PMID: 12847729 [PubMed - indexed for MEDLINE]

6: Williams TJ, Jose PJ. Related Articles, Links

Role of eotaxin and related CC chemokines in allergy and asthma.
Chem Immunol. 2000;78:166-77. Review. No abstract available.
PMID: 12847728 [PubMed - indexed for MEDLINE]

7: Askenase PW. Related Articles, Links

Proposing Th2 DTH relevant to asthma: cutaneous basophil hypersensitivity then and now.
Chem Immunol. 2000;78:112-23. Review. No abstract available.
PMID: 12847723 [PubMed - indexed for MEDLINE]

8: Smith SJ, Levi-Schaffer F. Related Articles, Links

Mast cell-eosinophil-fibroblast crosstalk in allergic inflammation.
Chem Immunol. 2000;78:81-92. Review. No abstract available.
PMID: 12847721 [PubMed - indexed for MEDLINE]

9: Robinson DS. Related Articles, Links

The Th1 and Th2 concept in atopic allergic disease.
Chem Immunol. 2000;78:50-61. Review. No abstract available.

EXHIBIT C

Annu. Rev. Biomed. Eng. 2002. 4:175–209
doi: 10.1146/annurev.bioeng.4.110701.120309

MECHANO-ELECTROCHEMICAL PROPERTIES OF ARTICULAR CARTILAGE: Their Inhomogeneities and Anisotropies

Van C. Mow and X. Edward Guo
Departments of Biomedical Engineering and Orthopaedic Surgery, Columbia University New York, New York 10027; e-mail: vcm1@columbia.edu, exg1@columbia.edu

Key Words cartilage, aggregate modulus, theoretical models, fixed charges, inhomogeneity

■ **Abstract** In this chapter, the recent advances in cartilage biomechanics and electromechanics are reviewed and summarized. Our emphasis is on the new experimental techniques in cartilage mechanical testing, new experimental and theoretical findings in cartilage biomechanics and electromechanics, and emerging theories and computational modeling of articular cartilage. The charged nature and depth-dependent inhomogeneity in mechano-electrochemical properties of articular cartilage are examined, and their importance in the normal and/or pathological structure-function relationships with cartilage is discussed, along with their pathophysiological implications. Developments in theoretical and computational models of articular cartilage are summarized, and their application in cartilage biomechanics and biology is reviewed. Future directions in cartilage biomechanics and mechano-biology research are proposed.

CONTENTS

1523-9829/02/0815-0175$14.00

INTRODUCTION: STRUCTURE AND COMPOSITION OF ARTICULAR CARTILAGE

Articular cartilage forms a thin tissue layer that lines the articulating ends of all diarthrodial joints in the body. The primary functions of this cartilage layer are to minimize contact stresses generated during joint loading and to contribute to lubrication mechanisms in the joint (1–3). A healthy joint is able to withstand the large forces associated with weight-bearing and joint motion over the lifetime of an individual. During pathologies such as osteoarthritis (OA), however, joint degeneration is characterized by cartilage and bony changes that lead to deformities, impaired joint motions, pain, and disability. The goal of many studies of cartilage mechanics over the years has been to determine the relationships between composition, structure (micro and macro), and material properties of healthy articular cartilage and, perhaps more importantly, to determine changes in its material properties associated with degeneration (1, 4–12). Herein some of the recent advances in cartilage biomechanics and function are reviewed and summarized. The emphasis of this review is on the new experimental techniques in cartilage mechanical testing, new experimental and theoretical findings in cartilage biomechanics and electromechanics, and emerging theories and computational modeling of articular cartilage. The charged nature and depth-dependent inhomogeneity in mechano-electrochemical (MEC) properties of articular cartilage are examined and their importance in the normal and/or pathological structure-function relationships of cartilage are discussed, along with their patho-physiological implications. Developments in theoretical and computational models of articular cartilage are summarized and their application in cartilage biomechanics and biology is reviewed. Future directions in cartilage biomechanics and mechano-biology research are proposed.

Articular cartilage can be considered a composite, organic solid matrix that is saturated with water and mobile ions (Figure 1). The water phase of cartilage constitutes averages from 65 to 80% of the total weight for normal tissue. This interstitial water is distributed non-uniformly with depth from the surface (6) and is an important constituent in controlling many physical properties (1–3). The dominant load-carrying structural components of the solid matrix by composition are the collagen molecules and the negatively charged proteoglycans (PGs). Collagen, on average, constitutes nearly 75% of the dry tissue weight; it assembles to form small fibrils and larger fibers with an exquisite architectural arrangement and with dimensions that vary through the depth of the cartilage layer (1, 8, 9, 13, 14). As with water, the distribution of collagen is stratified throughout the depth. The PGs of articular cartilage are biomacromolecules, which constitute 20%–30% of the solid matrix of cartilage by dry weight. A single PG aggrecan consists of a protein core to which numerous glycosaminoglycan (GAG) side chains are attached, with at least one negatively charged group, i.e., carboxyl and/or sulfate (15, 16). These charged groups give rise to a high-net negative charge density for the aggrecan that is quantified as the fixed charge density (FCD), or the number density of negative charges on a volume or weight basis (6, 17). Most aggrecan molecules

are further bound to a single hyaluronan chain of approximately 5×10^5 Da to form large PG aggregates of $50–100 \times 10^6$ Da (15, 16). The large size and complex structure of the PG aggregate immobilize and restrain the molecule within the intrafibrillar space, thus forming the solid matrix of articular cartilage (1–3, 15).

The solid matrix of articular cartilage has a highly specific ultrastructural (0.1–10 μm) arrangement consisting of successive zones from the articular surface to the subchondral bone interface (see Figure 1) (1, 9, 13, 14). Collagen fibrils in the superficial-most region [known as the superficial tangential zone (STZ)] of the cartilage layer are densely packed and oriented parallel to the articular surface. This collagenous membrane has a relatively low PG content and a lower permeability to fluid flow (18), which is important in providing for a barrier of high resistance against fluid flow when cartilage is compressed (10, 18). In the middle or transitional zone, the collagen fibers are larger and have been reported to be either randomly (1, 13, 19) or radially orientated (14, 20). In the middle zone, the PG content will rise from 10% (per dry weight) to 25%, giving rise to a high swelling pressure and water content, particularly in tissues with a damaged surface zone (6, 21). In the deepest zones, i.e., the zone nearest to the calcified cartilage and subchondral bone interface, the PG content is again lower (6), and the collagen fibers are larger and form bundles that are oriented perpendicular to the calcified/bony interface (13, 14, 20). The PG aggregates in this zone are larger and appear to be more saturated with aggrecan than in the surface or middle zones.

MECHANO-ELECTROCHEMICAL (MEC) BEHAVIOR OF ARTICULAR CARTILAGE

When an external load is applied to a diarthrodial joint, cartilage deforms to increase contact areas and local joint congruence (2, 3). As a result, a combination of tensile, shear, and compressive stresses is generated in the cartilage layer in a spatially varying distribution across the joint and through the cartilage thickness. The response of cartilage can be vastly different for compressive, tensile, and shearing stresses as a result of the specialized composition and structural organization of the cartilage layer. Furthermore, the response of the tissue to an applied load varies with time, giving rise to well-known viscoelastic behaviors such as creep and stress relaxation (Figure 2). There are two distinct dissipative mechanisms in response to loading responsible for the known viscoelastic behaviors: (*a*) the frictional drag force of interstitial fluid flow through the porous-permeable solid matrix (i.e., the flow-dependent mechanism); and (*b*) the time-dependent deformations of the solid macromolecules (i.e., the flow-independent mechanism). Because of the charged nature of articular cartilage and the electrolytes dissolved in the interstitial water, articular cartilage also exhibits complex electrochemical phenomena in addition to its mechanical response, including streaming and diffusion potential and charge-dependent osmotic swelling pressures (i.e., the Donnan osmotic pressure). New experimental techniques in cartilage mechanical testing, new experimental

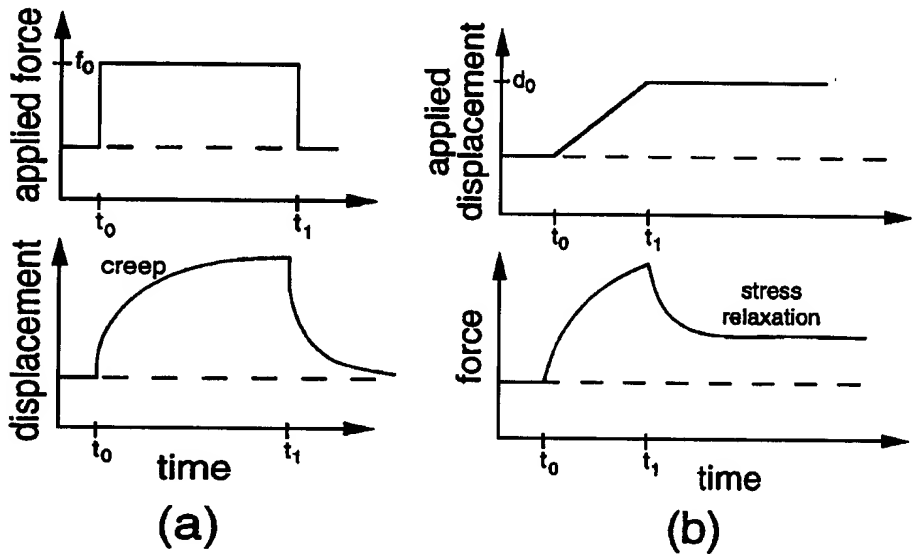

Figure 2 Schematics of load-deformation viscoelastic behaviors of articular cartilage. (*a*) In a creep test, a step force (f_0) applied onto a viscoelastic solid results in a transient increase of deformation or creep. In articular cartilage, this transient behavior is governed by the frictional forces generated as the interstitial fluid flows through the porous-permeable solid matrix and by the frictional interactions between the matrix macromolecules such as proteoglycan and collagen. Removal of f_0 at t_1 results in full recovery. In articular cartilage, recovery occurs as a result of the elasticity of the solid matrix and fluid imbibition. (*b*) In a stress-relaxation test, a displacement is applied at a constant rate, or ramped to t_0, until a desired level of compression is reached. This displacement results in a force-rise followed by a period of stress-relaxation for $t > t_1$, until an equilibrium force value is reached. In articular cartilage, the load rise is the result of the frictional forces of fluid flow and intermolecular interactions, and stress relaxation results from fluid redistribution within the tissue and to internal rearrangement of the molecular organization.

and theoretical findings in cartilage biomechanics and electro-mechanics are described below.

MECHANICAL PROPERTIES OF ARTICULAR CARTILAGE

The most frequently used testing configurations for compressive mechanical properties of articular cartilage are the confined compression, unconfined compression, and indentation tests (Figure 3*a*; *top*, *middle*, *bottom*, respectively). When cartilage is loaded in compression, a loss of tissue volume occurs owing to fluid exudation from the tissue. As indicated above, these effects give rise to significant time-dependent viscoelastic behaviors such as creep and stress relaxation. The

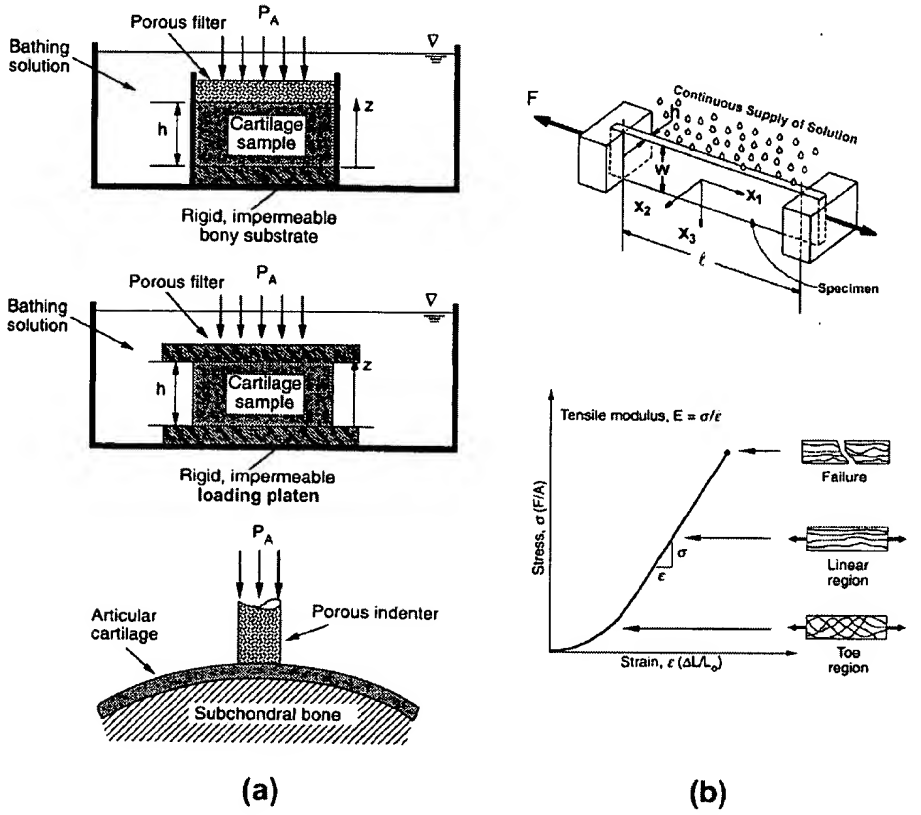

Figure 3 (*a*) Schematics of three configurations frequently used to study the compressive behavior of articular cartilage: the confined compression configurations (*top*), the unconfined compression (*middle*), and the indentation (*bottom*). (*b*) Schematics of the tensile testing of articular cartilage (*top*) and a characteristic stress-strain relationship for articular cartilage in a steady strain-rate tensile experiment.

movement of the interstitial fluid through the tissue is accompanied by high frictional drag forces between the fluid and the solid matrix and high pressures within the solid matrix (1, 5, 22–24). Thus, articular cartilage will creep in response to an applied constant compressive load (or stress) (Figure 2*a*) and exhibits stress relaxation in response to an applied constant compressive displacement (or strain) (Figure 2*b*). At equilibrium, no fluid flow or pressure gradients exist, and the entire load must therefore be borne by the solid matrix. It has been shown experimentally that for all cartilages tested to date, a remarkably linear relationship between the compressive stress and strain exists at equilibrium up to approximately 20% strain (22–24). Upon removal of the load or deformation, articular cartilage will recover its initial dimensions, largely through the elasticity of the solid matrix, the

increased osmotic pressure within the tissue, and the imbibition and redistribution of fluid within the interstitium (1, 22–26).

Because early studies showed that these time-dependent viscoelastic behaviors of articular cartilage seemed to be related to interstitial fluid flow and exudation (e.g., 6, 25), it was important to use an appropriate set of constitutive laws to describe the stress-strain behavior of this tissue that incorporates interstitial fluid flow and provides a method to measure the intrinsic compressive mechanical properties for the porous-permeable solid matrix. For these reasons, the biphasic mixture theory was introduced in 1980 to model articular cartilage as a mixture of an incompressible fluid phase and an incompressible solid phase that is porous and permeable. Also, the biphasic theory was to provide the theoretical framework to interpret the material property data obtained from experiments on articular cartilage (1, 5, 10, 22–24, 26)[1]. It was from this theory that the concept of intrinsic material properties of articular cartilage evolved (22). Because fluid pressure and internal frictional drag lead to much greater measures of load response by the tissue, it was shown that one can measure only the true mechanical properties of the collagen-PG solid matrix at equilibrium when the fluid pressure or frictional drag vanish. Many misinterpretations of cartilage material properties from earlier historical literature arose from a lack of understanding of this fundamental issue. The developments of constitutive theories for articular cartilage are reviewed below. The focus here is on the experimental determinations of intrinsic compressive properties of articular cartilage and other soft-hydrated tissues (1, 26, 27). In a stress-relaxation or creep test under confined compression, characterized by one-dimensional motion but multidimensional loading (due to the constraining sidewalls), two intrinsic material properties of articular cartilage can be determined: (*a*) the equilibrium confined compression aggregate modulus (H_A, in units of MPa or 10^6 Pa) and (*b*) hydraulic permeability (k, in units of $m^4/N \cdot s$), when an isotropic homogeneous biphasic constitutive theory (22) is employed to fit the transient stress-relaxation or creep response of the loaded specimen (1, 5, 22). At equilibrium, the deformation-load (or stress-strain) response gives a measure of the intrinsic compressive modulus (as defined above). The time course of the stress-relaxation (or creep) is determined by a characteristic time constant τ, which is defined by the compressive modulus (H_A), permeability (k) and thickness (h, or distance traveled by the fluid): $\tau = h^2/H_A k$. This time constant defines the characteristic gel-time of any porous-permeable elastic solid matrix and hence describes its time-dependent deformational behaviors such as stress-relaxation and creep (1, 22, 24). From this characteristic time constant τ and previously determined equilibrium compressive aggregate modulus H_A (plus the specimen geometry h), the hydraulic permeability k can be determined.

[1]Reference (22), where the biphasic theory was first introduced in 1980, is now the most frequently quoted paper ever published in the *Journal of Biomechanical Engineering*; this paper is also the recipient of the 1982 Melville Medal for the best contribution to the ASME archival literature.

The equilibrium compressive aggregate modulus for all types of articular cartilage ranges from 0.1–2.0 MPa; the hydraulic permeability is in the range of $(1.2–6.2) \times 10^{-16}$ m^4/N · s.

Fluid movements in cartilage loaded in compression are governed by the hydraulic permeability of the solid matrix. This permeability coefficient is in turn related to the extracellular matrix pore structure, apparent size, and connectivity (1, 6, 17, 22–24, 26–33). The concentration of PGs affects tissue permeability as the negative charges have been shown to impede hydraulic fluid flow (1, 6, 29–31); this effect is due to the electro-osmosis phenomenon that always acts to impede fluid flow (see below). In addition, the hydraulic permeability is related to the amount of compaction the tissue experiences, which results in an increase in the FCD and a decrease of apparent pore size (1, 6, 29–31). This nonlinear strain-dependent permeability function has been successfully modeled by the constitutive law $k = k_0 e^{M\varepsilon}$, where k_0 is the intrinsic permeability coefficient of uncompressed tissue, M is the dimensionless nonlinear interaction coefficient, and ε is the first invariant of the strain tensor (1, 22, 23, 31–33).

The permeability of normal cartilage is extremely small, thus indicating that in normal tissues large interstitial fluid pressures and dissipations are occurring during compression. These mechanisms for pressurization and high-energy dissipation provide an efficient method to shield the collagen-PG solid matrix from high stresses and strains associated with joint loading, because the pressurized fluid component provides for the major load-bearing function in cartilage (1, 34, 35). For example, under a confined compression test of articular cartilage, with simultaneous measurement of the interstitial fluid pressure at the specimen face, it was shown that the interstitial fluid immediately pressurizes upon loading and constitutes more than 95% of the total load support (34, 35). For normal articular cartilage compressive modulus and permeability, this high percentage of fluid load support can last more than 500 s due to its large characteristic time constant τ; hence for all practical purposes, in vivo, as a consequence of cartilage's intrinsic biphasic properties, the interstitial fluid shields the collagen-PG solid matrix from the high stresses that diarthrodial joints normally experience during the ordinary activities of daily living.

In a stress-relaxation or creep test in unconfined compression, the intrinsic equilibrium Young's modulus E, Poisson's ratio ν, and hydraulic permeability k can be determined assuming isotropic, homogeneous biphasic theory for articular cartilage (22, 36). Similar to the single-phase isotropic, homogeneous, linear elasticity theory, there are only two independent, intrinsic equilibrium elastic constants for a biphasic mixture: Young's modulus E and Poisson's ratio ν. These coefficients are related to other intrinsic, equilibrium elastic constants: shear modulus (μ) and aggregate modulus (H_A) by $\mu = \frac{E}{2(1+\nu)}$ and $H_A = \frac{E(1-\nu)}{(1+\nu)(1-2\nu)}$. The intrinsic, equilibrium Young's modulus of the solid matrix can be determined by the equilibrium response in the stress relaxation test, whereas the Poisson's ratio can be determined by two approaches: (*a*) measure directly from the unconfined tissue configuration using an optical method to determine the equilibrium lateral expansion during the

stress relaxation or creep test (36), or (*b*) use the master solution to calculate it from the biphasic indentation test (see below) (24, 36, 37). The intrinsic, equilibrium Young's modulus in compression ranges from 0.41 to 0.85 MPa; the intrinsic, equilibrium Poisson's ratio is in the range of 0.06 to 0.18 (37–42).

Another important testing technique for measuring compressive properties of articular cartilage is an indentation test (Figure 3*a*, *bottom*). Advantages of indentation tests on articular cartilage include a minimal disruption of normal articular cartilage microanatomy and the potential use in vivo (24, 38–42). However, an indentation test involves complex stress fields in articular cartilage under the indenter tip and within the tissue, and theoretical or numerical solutions of the indentation problem using appropriate constitutive laws for cartilage must be used to determine the intrinsic mechanical properties of articular cartilage and to interpret the data (24–26, 38–42). Again, using an isotropic, homogeneous biphasic theory for articular cartilage, the intrinsic, equilibrium aggregate modulus H_A, Poisson's ratio ν, and hydraulic permeability k can be determined simultaneously. The reported range from the combined theoretical and experimental studies falls within the same range measured by other techniques such as the unconfined compression discussed above [H_A, 0.4–0.9 MPa; ν, 0.13–0.45; and k, (4–10) $\times$ 10^{-16} $m^4/N \cdot s$]. Such cross-calibrations between different testing methodologies give confidence not only in the experimental methods, but also in the validity of the biphasic theoretical approach to describe the stress-strain behavior of articular cartilage.

When cartilage is tested in tension, the collagen fibrils and entangled PG molecules are aligned and stretched along the axis of loading (Figure 3*b*, *bottom*). For small deformations, when the tensile stress in the specimen is relatively small, a nonlinear toe-region is seen in the stress-strain curve owing primarily to collagen network realignment as it is pulled through the PG gel, rather than stretching of the collagen fibers.[2] For larger deformations, and after realignment, the collagen fibers are stretched and hence generate a larger tensile stress due to the intrinsic stiffness of the collagen fibrils themselves (4, 43–52). The proportionality constant in the linear region of the tensile stress-strain curve gives the intrinsic, tensile equilibrium Young's modulus, which is a measure of the flow-independent stiffness of the collagen-PG solid matrix, and it depends on the density of collagen fibers, fiber diameter and orientation, the type and amount of collagen cross-linking, and the strength of ionic bonds and frictional interactions between the permanent collagen network and the labile PG network. In general, the tensile modulus of healthy cartilage varies from 5 MPa to 25 MPa, depending on the location on the joint surface, and on depth and orientation of the test specimen relative to the joint surface. These well-known tensile properties clearly demonstrate the inhomogeneous and anisotropic nature of articular cartilage. For skeletally mature tissue, STZ articular cartilage specimens are much stiffer than middle and deep zone samples (4, 43–46), reflecting the effects of zonal collagen distribution. In

[2]There are no covalent bonds, nor are there any other permanent bonds between collagen and PGs; hence, collagen can easily slide through the PG gel when pulled.

addition, the tensile stiffness is greater for samples oriented parallel to the local split-line direction at the articular surface. These split-lines are presumed indicators of collagen fiber directions at the articular surface (1, 4, 43–46). However, for immature bovine specimens (from those joints with the presence of a growth plate), the tensile stiffness of the middle and deep zones is greater than that of the STZ specimens, possibly reflecting a different collagen ultrastructural organization in immature animals (45). For aging human articular cartilage, there is a general decline of the tensile modulus (4, 46, 49, 50).

Comparisons of tensile properties with compressive properties demonstrate a dramatic difference between the tensile and compressive elastic properties of collagenous tissues such as articular cartilage (1, 26). For example, Huang et al. (51, 52) performed uniaxial tensile tests of cartilage strips parallel and perpendicular to local split-line directions, as well as confined compressions along the depth direction of osteochondral plugs of human glenohumeral joint cartilage. In the limit of 0% strain in the toe region, the equilibrium tensile modulus on the humeral head STZ averages greater than 6.5 MPa along the collagen fiber direction and 4.5 MPa perpendicular to these directions, whereas the corresponding equilibrium compressive modulus averaged 0.5 MPa. At higher strains, the equilibrium tensile modulus can reach as high as 45 MPa and 25 MPa along parallel and perpendicular split-line directions, respectively. This two orders of magnitude difference in the tension and compression moduli clearly demonstrate the tension-compression nonlinear behavior of articular cartilage; using the recently developed conewise material symmetry model in the biphasic constitutive equation, this phenomenon has been extensively and carefully studied (51–54). The conewise biphasic theory provides remarkable accuracy in describing a large variety of tensile and compressive behaviors known to exist for articular cartilage.

In the third direction, articular cartilage appears to exhibit anisotropic mechanical properties as well. The early studies on articular cartilage anisotropy mainly emphasized the uniaxial tensile experiments in the articular surface plane and parallel and perpendicular to the split-line directions (43–46). These studies showed that the tensile modulus in the direction parallel to the split-line is always greater than that in the perpendicular direction, usually by more than a factor of two. Based on anisotropic swelling studies, however, it is likely that the tensile modulus in the third direction (i.e., radial direction—perpendicular to the surface) is even less, although hard experimental evidence is difficult to obtain (55, 56).

Because the tensile properties of cartilage differ along these three mutually perpendicular directions, the elastic material symmetry of cartilage is at least orthotropic, with its three planes of symmetry defined in situ by the split-line direction in a plane tangent to the surface (1-direction), the direction perpendicular to the split-line direction in the same tangent plane (2-direction), and the direction normal to this plane (3-direction), i.e., the radial (or depth) direction of the cartilage layer. Existing literature also supports cartilage anisotropy in tension in measurements of Poisson's ratio for cartilage in uniaxial tension. For human humeral head cartilage, Huang et al. (52) reported an average Poisson's ratio value of $\nu_{12} = 1.3$ for

uniaxial tension along the 1-direction and measurement of the contraction along the 2-direction, and a similar average of $\nu_{21} = 1.3$ for the converse configuration, in the STZ of adult articular cartilage; in the middle zone, these values reduced to $\nu_{12} = 1.2$ and $\nu_{21} = 1.0$.

In contrast to tensile measurements, only a limited number of studies on the anisotropy of cartilage in compression are reported. Recently, using a new optical technique and incorporating a conewise tension-compression nonlinear biphasic mixture theory, Wang et al. tested small cubic cartilage specimens in three directions (57). Their results demonstrated that neither the Young's modulus nor the Poisson's ratio exhibits the same values when measured along these three loading directions (Figure 4). These studies also suggest that a constitutive framework that accounts for the distinctly different responses of cartilage in tension and compression is more suitable for describing the equilibrium response of cartilage; within this context, cartilage exhibits no lower than orthotropic symmetry.

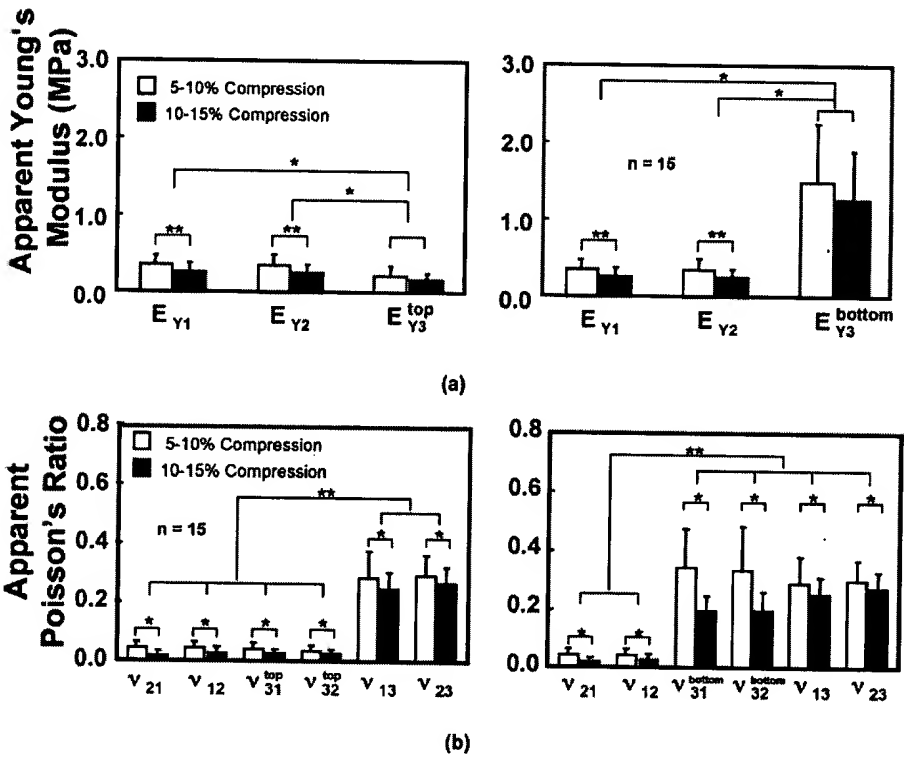

Figure 4 (*a*) The apparent Young's moduli and (*b*) the apparent Poisson's ratios determined for the three directions: along split lines, perpendicular to split lines, and in the depth, at two compression levels and at both the top and bottom zones (*left* and *right*, respectively) along with results of statistical comparisons ($^*p < 0.01$; $^{**}p < 0.001$). [Modified from (57)].

Mechano-Electrochemical Properties of Articular Cartilage: Effects of Fixed Charges

Increase of tissue hydration and loss of proteoglycans are the earliest signs of articular cartilage degeneration during OA (1, 4–7, 46, 56, 58, 59). For this reason an understanding of the mechanisms for swelling and development of methods to quantify cartilage swelling have been of great interest for many years. Swelling in cartilage arises from the presence of a high density of negatively charged PG molecules. Each PG-associated negative charge requires a mobile counter-ion (e.g., Na^+) that is dissolved within the interstitial fluid to maintain electro-neutrality within the interstitium (6). This gives rise to an imbalance of mobile ions between interstitium and the external bathing solution. This excess of mobile ions colligatively yields a swelling pressure (6, 17, 57–65) that contributes to the swelling pressures in articular cartilage and its hydrophilic nature. The swelling pressure that is associated with the FCD is known as the Donnan osmotic pressure (6, 59–65).

At equilibrium, the swelling pressure in articular cartilage is balanced by tensile forces generated in the collagen network (6, 64) or, in a mathematically more rigorous and accurate description, balanced by the stresses developed in the load-bearing components of solid matrix (1, 50–62). Therefore, at physiological concentrations, the charged solid matrix of cartilage, even when unloaded, is in a state of pre-stress. This balance of the Donnan osmotic swelling pressure and the constraining matrix stress determines the dimensions and hence the equilibrium hydration of the cartilage. Thus, changes in this internal swelling pressure, arising from altered ion concentrations of the external bath, or changes in the internal GAG content will result in changes in tissue dimensions and hydration. In addition, the combined variation in GAG concentration and matrix stiffness through the cartilage layer will cause nonuniform swelling through the depth and give rise to a warping or curling effect (10, 55, 56).

The swelling behaviors of cartilage have long been observed as a swelling of the tissue in hypotonic salt solution or a shrinkage of the tissue in hypertonic salt solutions. In early studies (6, 58), samples of cartilage were weighed immediately after excision and again after equilibration in a physiological test bath (0.15 M NaCl). No significant change was found in the tissue weight of normal human cartilage from its in situ value after soaking in the solution. However, a large weight gain was observed in slices of human OA articular cartilage ($\sim$300 μm) after equilibration in 0.015 M NaCl compared with 0.15 M NaCl. The largest gain in water was $\sim$20% in slices from the middle zone of cartilage, where the FCD is known to be largest (see Figure 1*d*). In the same studies, cartilage samples incubated with collagenase (thereby loosening the collagen network) gained significantly greater amounts of water than normal cartilage, a finding that has been corroborated in later studies of bovine cartilage (56, 58, 65). These studies demonstrate that integrity of the collagen network is important for resisting the swelling pressures in articular cartilage and that a damaged collagen network is associated with increased hydration.

In addition to techniques designed to quantify dimensional or weight changes of cartilage, swelling behaviors have been studied in isometric tensile and compression swelling experiments (4, 46, 55, 60, 66). In these tests, samples of cartilage are held at a fixed length with some initial tensile (or compressive) strain and subjected to a change in the ionic environment of the bathing solution. The transient force recorded at the sample grips increases in response to a solution change from 0.15 M NaCl to hypotonic solution, which gives evidence of an increase in interstitial Donnan swelling pressure. The ratio of the equilibrium tensile stresses in two varying osmotic environments, as well as the time constant that characterizes the stress decay, have been quantified for cartilage (4, 55, 66). This characteristic time constant is identical to τ given above, except that the permeability coefficient is now replaced by the diffusion coefficient. Importantly, these studies have demonstrated that the characteristics of swelling in the isometric tension test are highly dependent on the ratio of collagen to PG and PG concentration alone. This dependence also reflects the balance between collagen network forces and the interstitial swelling pressure, which governs the swelling mechanism in articular cartilage.

The negative charges of the proteoglycans are also the source of all the known electrochemical events in the cartilage (1, 6, 17, 30, 31 , 60, 62, 67–74). By virtue of the electro-neutrality law, there is always a cloud of counter-ions (e.g., Ca^{2+}, Na^{+}) and co-ions (e.g., Cl^{-}) dissolved in the interstitial water surrounding these fixed charges on the proteoglycans. Unlike the fixed charges, however, these ions are free to move with the interstitial fluid by convection and through the interstitial fluid by diffusion. These fixed charges can profoundly affect not only tissue hydration and control of fluid content but also ion transport through the interstitium, and also a broad spectrum of other observed MEC responses, such as electric potential and current, and the measured apparent material properties of the tissue (71–74).

Recent theoretical analyses using a triphasic mixture theory have identified two important sources of electrical potential in the negatively charged articular cartilage: a diffusion potential resulting from the inhomogeneous distribution of the fixed charge density—either strain-induced or naturally occurring (1, 6, 50, 62, 75)—and a streaming potential resulting from fluid flow within charged tissue (17, 60, 61, 67, 70–74). These two sources of electrical potentials have an opposite polarity and compete against each other depending on the intrinsic mechanical stiffness and fixed charged density in the tissue. Only a very limited number of experimental studies have focused on the MEC behaviors of articular cartilage. However, these recent theoretical studies indicate that the charged nature of articular cartilage has a profound influence not only on the swelling and electric behaviors but also on mechanical behaviors as well, which is reviewed below in the sections on theories of articular cartilage.

Depth-Dependent Inhomogeneity of Articular Cartilage Properties

The heterogeneous composition and micro-structural organization of cartilage tissue (Figure1) strongly suggest that there must also be some intrinsic

inhomogeneities of the MEC properties. For example, the inhomogeneous distribution of proteoglycans must have resulted in an inhomogeneous distribution of FCD through the depth of the tissue (e.g., 6, 75). This depth-dependent inhomogeneous FCD has been shown to affect the magnitude of the internal electrical potential and current within the interstitium where chondrocytes reside (60, 62, 74–77). As discussed above, these depth-dependent FCD inhomogeneities may have profound effects similar to the spatial variations that collagen composition and ultrastructure have on the tensile properties (43–52). The nature and magnitudes of MEC signals transmitted to the chondrocytes in situ, and thus to the cell nucleus, are all determined by the mechanical and physicochemical properties of the extracellular matrix and that of the pericellular matrix (68, 76–80). Indeed, all these MEC events have to be affected by the compositional and material inhomogeneities of the tissue.

Recent developments of new experimental methodologies have provided additional information about cartilage material inhomogeneities in compression and the deformational behavior of chondrocytes under loading (56, 57, 76–84). For example, with the help of video microscopy, the fluorescently labeled chondrocyte nuclei have been used as the fiducial markers to quantify the inhomogeneous equilibrium strain fields within articular cartilage during confined compression (Figure 5). Using these strain fields (81, 82), together with applied loads, the depth-dependent equilibrium compressive aggregate modulus distributions have been determined for the cartilage modeled as an isotropic, inhomogeneous, biphasic material (83, 84). These results gave an intrinsic aggregate modulus of 1.16 MPa in the superficial layer and 7.75 MPa in the deep layer (83). Recently, Wang et al. (83, 84) extended the video microscopy technique developed by Schinagl et al. (81, 82) by incorporating an optimized digital image correlation technique (using a thin plate-spline smoothing technique) and the results of the triphasic theory (60–62) to allow the determination of a continuous depth-dependent distribution of the aggregate modulus and FCD (83, 84). This remarkable breakthrough allowed a non-invasive methodology to determine the intrinsic compressive stiffness (H_A) of the extracellular matrix and the depth-dependent inhomogeneous FCD distribution for articular cartilage (84) (Figure 5). The intrinsic compressive stiffness of the solid matrix and FCD are shown in Figure 5. For qualitative comparison, the mean FCDs determined from biochemical analyses of the three zones are top slices (the surface zone), 0.098 $\pm$ 0.016 mEq/ml; the middle slices, 0.112 $\pm$ 0.019 mEq/ml; and bottom slices (the deep zone), 0.132 $\pm$ 0.063 mEq/ml. These comparisons are very favorable (6, 65).

Although surface-to-surface measurements (such as the confined aggregate modulus or surface-to-surface applied strain) provide bulk properties or bulk characterization of a tissue, they provide only indirect insights into the internal deformational behavior of the inhomogeneous tissue. Quantitative analyses of the spatial and temporal gradients of strain, pressure, osmotic pressure, and electric potentials around chondrocytes require detailed knowledge of the depth-dependent material properties. From numerous in vivo (animal models of OA) and in vitro (explant or cell culture) studies, it is known that these cells can sense biomechanical stimuli

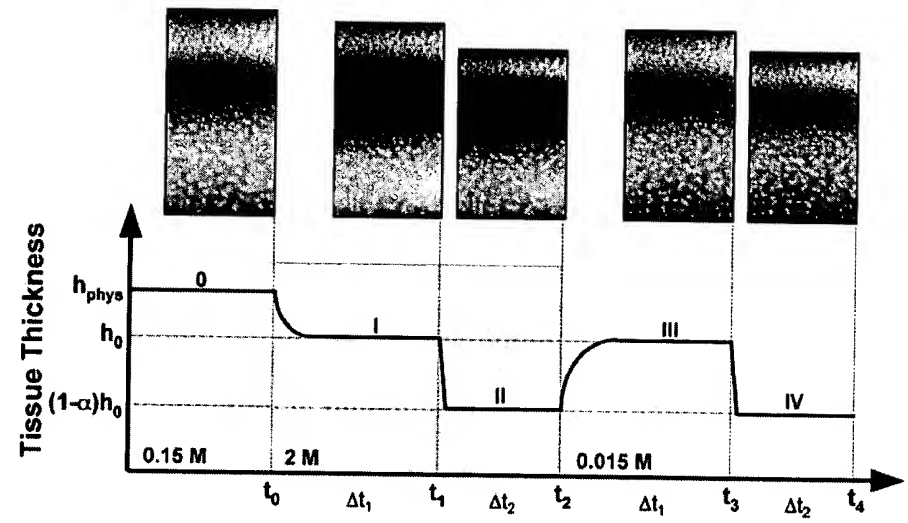

(a)

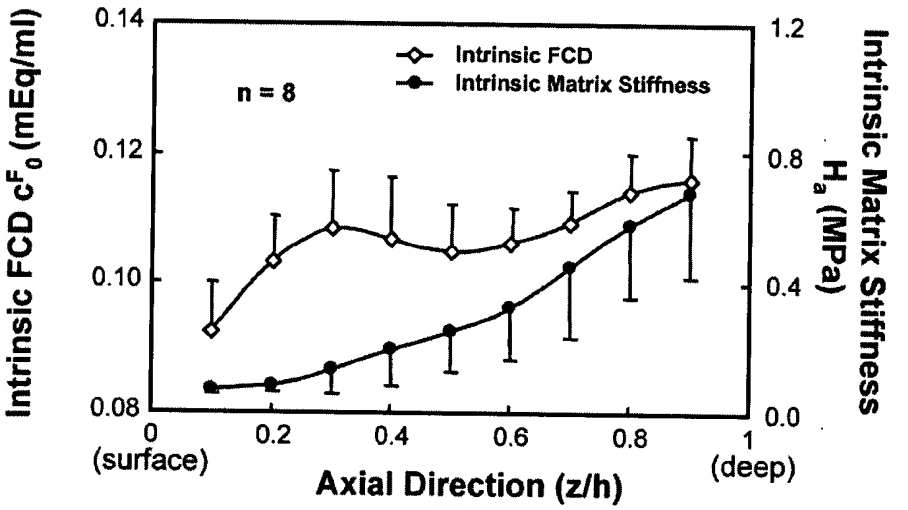

(b)

Figure 5 (*a*) Experimental protocol for determination of the depth-dependent intrinsic solid matrix stiffness [$H_a(z)$] and intrinsic fixed charge density (c_0^F). In the plot of the tissue thickness versus time, the shaded areas represent various NaCl concentrations, where h_{phys} is the initial thickness of the tissue specimen in physiological saline (0.15 M NaCl), h_0 is the initial thickness of the tissue specimen in 2 M NaCl, and $(1-\alpha)h_0$ is the tissue thickness after applied compression. The curved portions of the plot represent either shrinking or swelling after changing NaCl concentration; the ramps represent stress-relaxation experiments in either 2 M NaCl or 0.015 M NaCl. (*b*) The resulting distribution of the intrinsic fixed charged density and intrinsic matrix stiffness.

(e.g., 68, 75, 85–92) in their immediate environ. Indeed, joint immobilization and altered loading are also important factors in maintaining a healthy tissue (e.g., 7, 56, 93, 94). Therefore, it is important to know the exact nature of the MEC signals in the neighborhood of the cell; only in this manner can we learn how the signal transduction process takes place and how it is related to changes in cell biosynthetic and catabolic activities.

STRUCTURE-FUNCTION OF ARTICULAR CARTILAGE

In previous sections, we reviewed several of the basic known MEC properties of articular cartilage. Some of these properties are important in understanding how articular cartilage functions as the bearing and lubricating materials in all diarthrodial joints. To appreciate the capacity of articular cartilage to support mechanical load, for example, one study has reported that compressive stresses as high as 20 MPa exist in the hip (approximately 3000 pounds per square inch) (95). Such high compressive stresses can easily crush muscles, tendons, and ligaments. How then can cartilage survive in these severe loading conditions? Answers come from the multiphasic nature of articular cartilage. Because of the relatively low permeability of the porous-permeable extracellular matrix of cartilage, it is very difficult for the interstitial fluid to escape from the tissue under mechanical loading (1–3, 10, 22, 23, 26, 29, 32–36, 95–98). Therefore, fluid pressurization built up in cartilage contributes to the majority of the load support in cartilage. Indeed, recent studies have quantified directly the fluid pressure in cartilage and report that the fluid pressure supports up to 95% of the applied load, whereas the remaining 5% is supported by the contacting collagen and PG matrix of the opposing articular surface (34, 35).

The mechanism of fluid pressurization not only contributes to the remarkable load support capacity of diarthrodial joints but also is the key to the understanding of the extremely low-friction coefficient in the joint lubrication of cartilage (1–3, 34, 35, 96, 97). The friction coefficient of cartilage surface is 20 times smaller (5%) than that if the entire load were supported by the collagen and PG extracellular matrix, as would be the case if interstitial fluid pressurization did not exist. Alterations in mechanical properties of cartilage such as decreased elastic modulus and increased hydraulic permeability, as well as micro-structural changes such as surface fibrillations or fissure, all lead to a compromised load support mechanism in cartilage, especially the loss of fluid pressurization (3, 9, 10, 18, 22, 29, 94). The consequence is an increased frictional coefficient of the joint, which would further impose detrimental higher shear stresses on the already damaged extracellular matrix of cartilage, leading to continuing and accelerated deterioration of its mechanical properties.

Articular cartilage, a metabolically active tissue, is synthesized, organized, and maintained by the terminally differentiated chondrocytes that make up less than 10% of the matrix by volume and/or weight (6, 15, 80, 91). The composition and organizational structure of the extracellular matrix shield the ensconced chondrocytes

from the high stresses and strains generated by joint loading and motion, although not completely isolating the cells from their mechanical environment (75–94). The extracellular matrix, with associated interstitial fluid, solutes, and ions, can collectively be thought of as a mechanical signal transducer that receives input in the form of joint loading and yields an output of various extracellular signals (e.g., deformation, pressure, electrical), as well as fluid, solute (e.g., nutrient), and ion flow fields (76). The predominant mechanical signal in situ for normal articular cartilage is hydraulic pressure (95% of the total applied load). The remaining 5% of loading must act on the extracellular matrix, and because it is very soft, the matrix can also experience considerable amounts of stretch, compression, and shear. A deformation-enhanced FCD inhomogeneity also amplifies the electromechanical events within the extracellular matrix (76–79, 86, 91). All these signals in turn define the MEC milieu for the chondrocytes in situ and may act independently or in combination to influence activities of the chondrocytes, or alternatively, may be ignored by the chondrocytes.

The mechanism(s) by which chondrocytes convert physical stimuli to intracellular signals (e.g., mechano-transduction in the case of mechanical stimuli), which in turn direct cell synthetic activities, represents an area of intense current orthopedic and biomedical science research. An important step toward the identification of these mechanisms must necessarily be an accurate description of the nature of the MEC environment around chondrocytes in situ. From the engineering perspective, one challenge to defining the chondrocyte MEC environment is the development of detailed and accurate constitutive laws for articular cartilage and chondrocytes. Such constitutive laws, with all kinds of possible MEC properties and external loading as inputs, are necessary to describe the required spatial and temporal MEC events, such as the states of stress, strain, pressures (osmotic and hydrodynamic), fluid and ion flows, and streaming potentials/currents, within articular cartilage (Figure 6). Clearly this information is needed for understanding the signal transduction mechanisms in cartilage.

An important consideration in functions of articular cartilage is the natural inhomogeneity in mechanical properties of cartilage from cartilage surface to the underlying subchondral bone. As indicated above, the composition and structure of cartilage vary through the depth of the tissue (Figure 1). Not surprisingly, the mechanical properties of cartilage also vary through the depth (Figure 5). This natural inhomogeneity of mechanical properties in the normal articular cartilage may play an important role in augmenting the signal transduction mechanisms to the chondrocytes in order to maintain the integrity of the extracellular matrix of cartilage. It is a fundamental hypothesis that in order to fully recover and sustain load-bearing and lubrication functions of articular cartilage, which have been lost through OA or injuries, the natural distribution of the biochemical composition, micro-structural organization, and MEC properties of the tissue must be restored (7). How to do this remains a difficult and challenging task for orthopedic research (99).

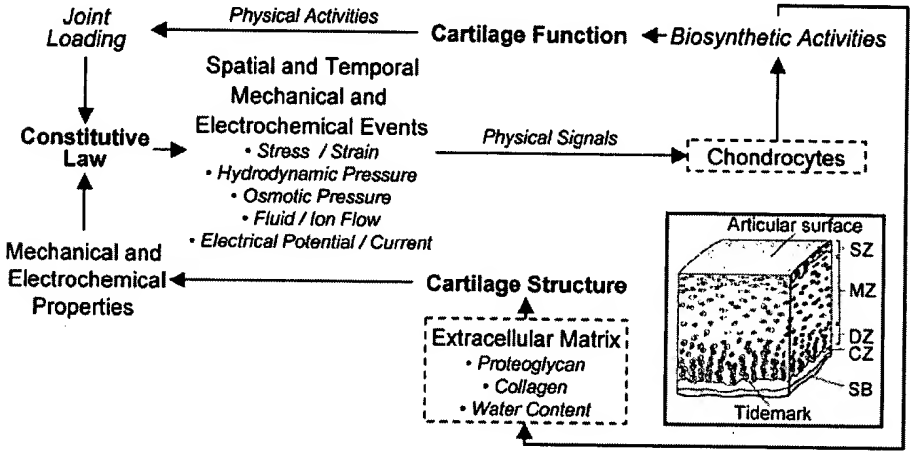

Figure 6 Diagram of articular cartilage structure and function, chondrocyte distribution, and the inter-relationships between composition, mechano-electrochemical signals, and chondrocyte biosynthetic activities.

THEORETICAL AND COMPUTATIONAL MODELING OF ARTICULAR CARTILAGE

Salient viscoelastic, nonlinear, inhomogeneous, and anisotropic properties of articular cartilage have motivated the developments of physiologically realistic, and mathematically rigorous and accurate constitutive laws describing the stress-strain behaviors of cartilage that can be used to analyze the complex MEC behaviors within the tissue (22, 31, 32, 60–62)[3]. These constitutive laws provide a set of physically meaningful and measurable mechanical and electrochemical material parameters that are needed for defining cartilage properties; this is especially important in extracting the relevant material properties from articular cartilage, or from any other soft, hydrated-charged connective tissues, in simple testing configurations. First, these testing configurations are crucial in quantifying functional relationships for articular cartilage in normal and diseased states such as in osteoarthritis or for evaluating the functional capacity of newly engineered cartilage constructs (99). It is also important that any constitutive theory has to be validated by a variety of experiments. Second, defining the chondrocytes MEC environments also requires the development of detailed and accurate computational methods that incorporate these constitutive laws (e.g., 73, 74, 78, 83, 89, 100–102). Furthermore, all diarthrodial joints have a complex three-dimensional geometry. Thus it requires

[3]Reference (60) introduced the triphasic theory and was the recipient of the 1992 best paper award from the Bioengineering Division of ASME.

the developments of efficient computational techniques employing these various constitutive laws, as well as accurate anatomic geometries (e.g., 103–105), and the high physiological loading levels (e.g., 2, 3, 95, 98, 106).

Many constitutive theories developed and used since the 1940s include both linear and nonlinear elasticity and viscoelasticity theories of various forms and infinitesimal and finite deformation theories; in addition various material anisotropies and inhomogeneities have been proposed. This review focuses mainly on the multiphasic porous media theories (e.g., 22–24, 29–35, 61, 62, 73, 74, 77, 78, 83, 84), in which the material constants in the theory have clear meanings and have been or can be measured experimentally.

There are also several microstructural theories of composite materials (e.g., 107–110) based on the microstructural organization of articular cartilage and cells. These microstructural theories are interesting scenarios, but the challenges lie in a complete description of the complex microstructures of the tissue or cell; i.e., they should have a significant range of validity and there should be independent and objective methods to determine the material constants needed to define the deformational behaviors of the tissue before they can be used as predictive models. Thus herein, we emphasize the two types of continuum theories commonly used to describe the deformational behaviors of these biological tissues: (*a*) the biphasic mixture theories of hydrated soft tissues (e.g., 1, 22–24, 29, 32–35, 78) and (*b*) the multiphasic mixture theories for electrically charged hydrated soft tissues (e.g., 30, 31, 60–62, 73, 74, 77) that include dissolved ionic species in the interstitial fluid. The focus is on the recent advances in the use of continuum mixture theories to model these types of biological tissues.

Biphasic Mixture Theory of Articular Cartilage

The biphasic theory assumes that articular cartilage is composed of two intrinsically incompressible phases: an interstitial fluid phase and elastic solid matrix phase. The solid matrix phase consists of a porous-permeable, elastic-solid matrix of collagen type II fibers and PG aggregates. The theory takes the consideration that the load support in articular cartilage derives from the fluid pressure in the interstitial fluid phase and the elastic stress developed within the solid matrix during loading (22). The movement of water through this porous-permeable solid matrix is mainly governed by the frictional drag between solid-fluid interface of the micro-pores. Since its appearance in 1980, this biphasic mixture theory for articular cartilage has been applied in various experimental and theoretical studies of this material (see review articles 1–3, 26). Over the years, these studies have included experimental determinations of cartilage mechanical properties in (*a*) confined compression of articular cartilage (1, 5, 11, 22, 32, 34, 61, 83), (*b*) unconfined compression of articular cartilage (36, 37, 51, 52, 74, 101, 102), (*c*) in situ indentation of articular cartilage (24, 38–42, 87, 88), (*d*) contact analyses of articular cartilage surfaces (1, 2, 26, 100, 111–113), and (*e*) chondrocyte-matrix interaction under mechanical loading (78, 86, 88, 114). The numerical methods for finite

element formulation using the biphasic theory have been developed by Spilker and colleagues and applied to indentation and unconfined compression tests of cartilage samples, as well as the chondrocyte-matrix interaction under loading (2, 100, 114–120). Recently, a commercial finite element software such as ABAQUS, using an equivalent poroelastic formulation, predicted computational results consistent with those biphasic finite element analyses (119). Therefore, one may choose to use a finite element software that offers equivalent formulation as biphasic theory for cartilage mechanics studies. However, care must be exercised to make clear the theoretical consistency of the mixture theory approach (biphasic or triphasic) used in an application versus that of the poroelasticity approach (121, 122).

The early success of the isotropic, homogeneous form of biphasic mixture theory in confined compression of articular cartilage encounters some difficulties in predicting viscoelastic behaviors of articular cartilage in testing configurations other than confined compression, for example, unconfined or indentation experiments (36, 101, 102, 115). This should not come as a surprise because one knows that articular cartilage is an inhomogeneous, nonlinear, and anisotropic material and that the frictionless boundary conditions imposed may not be experimentally attainable. Recent advances employing higher levels of tissue material complexities have been theoretically modeled, including inhomogeneities in material properties and FCD (75, 77, 78, 81–84), material symmetries (transverse isotropy and conewise tension-compression nonlinearities), and matrix viscoelasticities (43–46, 52–55, 69, 70, 92, 101, 102, 120). These studies have made some exciting enhancements in the ability of the biphasic mixture theory to model and describe the interstitial mechanical and electrochemical stimuli around chondrocytes.

The incorporation of a transverse isotropy material tensor into the linearly elastic, homogeneous, biphasic formulation improved the predictive power in unconfined compression analysis (120) and significantly changed the stress field within articular cartilage in a contact problem (92, 100), whereas the inclusion of intrinsic matrix viscoelastic properties for the solid matrix in the biphasic theory (123) improved the prediction in the unconfined compression, as well as material property determinations (10, 51–54, 101, 102). Other efforts of modeling cartilage including the introduction of a fibrous microstructure into the linearly elastic biphasic theory demonstrated good agreements between the theoretical prediction and experimental data in unconfined compression (124). Most recent studies that have incorporated conewise tension-compression nonlinearity (53) and intrinsic viscoelasticity (124) into the solid matrix behavior of the biphasic theory have demonstrated remarkable accuracy in the modeling articular cartilage deformational behaviors (51, 52, 54). Furthermore, the prediction of their theory in fluid pressure (34, 35) in confined compression fits well the independent measurements of fluid pressure, thus providing further confidence in the ability of the biphasic theory to model a variety of deformational behavior commonly exhibited by soft, hydrated connective tissues.

The classical biphasic theory (22) also cannot predict successfully the tensile viscoelastic responses of articular cartilage (4, 43–50). It is clear that cartilage

exhibits tension-compression nonlinearity and flow-independent viscoelasticity (44, 48). The theoretical prediction of the biphasic-conewise linear elasticity model cannot describe the viscoelastic response of cartilage under uniaxial tension as well (51). This suggests that the intrinsic viscoelasticity (flow-independent) of the solid matrix (10, 48, 123, 125, 126) must be manifesting its known viscoelastic behavior during tensile tests (51, 52). This is consistent with the microstructure and composition of articular cartilage. When cartilage is loaded in tension, collagen fibers are the predominate structural components withstanding the stretch, whereas fluid flow and pressurization are the more predominate feature in compression. This probably also explains why the biphasic mixture theory, including solid matrix viscoelasticity, is a better predictor of cartilage response in the unconfined compression test. Indeed, the biphasic, conewise (i.e., the bi-linear, stress-strain behavior) elasticity, quasi-linear viscoelasticity (biphasic-CLE-QLV) theory can predict cartilage tensile responses extremely well in addition to behaviors in both confined and unconfined compression (51, 52). These added levels of modeling sophistication within the constitutive context of a biphasic mixture theory have the enhanced predictive power to describe a variety of testing configurations and confirm the notion that articular cartilage is a mixture-type material that is nonlinear, viscoelastic, and anisotropic.

The power of a constitutive model such as the biphasic mixture theory lies not only in the characterization of material properties of articular cartilage but also in its predictive ability that cannot be obtained from experimental studies or from any existing micro-structural models. For example, a biphasic cell-matrix interaction model has recently been developed to predict mechanical (fluid and solid) interactions in cartilage during compression and thus provide an in-depth understanding of the mechanical environment for chondrocytes toward the elucidation of mechano-signal transduction for metabolic functions (e.g., 78, 79, 86, 91, 114, 127). The mechanical environment at the cellular level was found to be time-varying and inhomogeneous, and the large difference (approximately 3 orders of magnitude) in the elastic properties of the chondrocyte and those of the extracellular matrix results in stress concentrations at the cell-matrix interface that showed a nearly twofold increase in strain and dilatation (volume change) at the cellular level, compared with the macroscopic level (Figure 7) (78, 114). The presence of a narrow pericellular matrix with properties that differed from those of the chondrocyte or extracellular matrix significantly altered the principal stress and strain magnitudes and directions within the chondrocyte, suggesting a major functional biomechanical role for the pericellular matrix (78, 127). These findings suggest that even under simple one-dimensional compressive loading conditions, chondrocytes are subjected to a complex local mechanical environment consisting of tension, compression, shear, and fluid pressure and flow. Clearly then, knowledge of the local stress and strain fields in the extracellular matrix is an important step in the interpretation of studies of mechano-signal transduction in cartilage explant culture models. Another good example for use of the biphasic mixture theory is that it can be easily adapted to incorporate the inhomogeneous distribution of

aggregate modulus to predict the exact distributions of stress, strain, fluid flow and pressure fields inside a cartilage sample (81–84). Therefore, the contribution of tissue inhomogeneity toward modulating mechanical environment around chondrocytes inside articular cartilage is now possible. Additional examples are given below, while the experimentally derived inhomogeneous distributions of both aggregate modulus and FCD will be incorporated in a triphasic mixture model of articular cartilage (60).

Multiphasic Mixture Theory of Articular Cartilage

Because the large negatively charged PG aggregates have much less mobility than that of dissolved electrolytes in the interstitial water, these charges can be considered as fixed onto the collagen-PG solid matrix (6, 15, 17, 60, 64). According to the Donnan equilibrium ion distribution law (6, 60, 63), the fixed charges attract mobile counter-ions that collectively give rise to a swelling pressure within the tissue, i.e., the Donnan osmotic pressure. The ions, together with the fixed charges, are also responsible for a series of electrochemical responses known to be exhibited by cartilage under loading (1, 6, 17, 27, 30, 31, 67–74, 128–130). These studies showed that each phase (the charged solid matrix, water and ions) of the articular cartilage contributes to its compressive, tensile, electrokinetic, and transport behaviors. It had been well known for over a decade that a broader foundation was needed to provide a unified theoretical view encompassing the widely disparate interpretations of cartilage physicochemical and swelling properties, mechanical behaviors, and electromechanical effects. In the past decade, a number of constitutive theories for articular cartilage and other charged connective tissues (e.g., the intervertebral disc) have been developed using the multiphasic perspective to account for the known electrical phenomena (1, 27, 60–62, 67, 71–74). These theories can be summarized in the following categories: (*a*) triphasic mixture theory (60–62, 73, 74), (*b*) quadriphasic theory (71, 72), and (*c*) the ad hoc or structural electromechanical theories (55, 67, 129–131). The triphasic mixture theory for charged hydrated tissues was developed by Lai et al. in 1991 (60), and the equivalent quadriphasic theories were developed by Huyghe & Janssen in 1997 (71). In essence, the difference between these two theories is in the counting of phases, i.e., whether one should consider Na^+ and Cl^- as one or two phases; in the triphasic theory Na^+ and Cl^- are considered as two ionic species of the third phase.[4] In this manner, the triphasic theory can accommodate many species such as the multi-electrolyte theory developed by Gu et al. (31). This theory has provided the thermodynamic foundation for the well-known Hodgkin-Huxley equation of membrane electric potentials. For both theories, finite element formulations have been developed for potential complex mechanical/chemical loading configurations (72–74).

[4]It is of interest to note that in the 1980s, the attempts in theoretical continuum modeling of cartilage electro-mechanical (e.g., 67, 131) or chemo-mechanical (e.g., 55) phenomena have no fixed charges associated with the solid matrix, nor ions in the interstitial fluid (67, 131).

The triphasic theory and its extension to incorporate multiple species of the ion phase have been used to describe the flow-dependent and flow-independent viscoelastic behaviors, swelling behaviors, and electrokinetic behaviors of charged, hydrated soft tissues (1, 27, 60–62, 67, 71–74). For example, electrokinetic behaviors of charged, hydrated soft tissue under pressure-differential-induced permeation are related to the balance of convective transport of ions through the tissue under zero current condition, in accordance with the phenomenological theory (6, 17, 67, 131, 132), using electrokinetic coefficients. However, these electrokinetic coefficients are not easily related to physical parameters such as FCD, molar concentration of the ions, and frictional coefficients between ions/fluid and the solid matrix. Using the triphasic theory, explicit expressions among those electrokinetic coefficients and the physical parameters of the charged tissue have been derived (30, 31, 60–62). The triphasic analysis of the stress relaxation test of cartilage tissue in confined compression clearly demonstrates the contribution of the FCD in the MEC behaviors of a charged, hydrated soft tissue under compressive loading (61, 62). The results show that the apparent equilibrium aggregate modulus, which can be routinely determined from the biphasic mixture theory, actually consists of two parts: the Donnan osmotic pressure and the intrinsic stiffness of an uncharged matrix. Contrary to former popular belief, on 100% load support (6), the Donnan osmotic pressure contributes up to only approximately 50% of the equilibrium-confined compression stiffness (61) and approximately 30% in unconfined compression (74). Furthermore, recent theoretical analyses using a triphasic mixture theory identified the two important sources of electrical potential in negatively charged articular cartilage: a diffusion potential resulting from the inhomogeneous distribution of the FCD (either strain-dependent or naturally occurring) and a streaming potential resulting from fluid flow convection within charged tissue. These two sources of electrical potentials have an opposite polarity and compete with each other depending on the intrinsic mechanical stiffness and fixed charged density in the tissue (62).

Using a finite element formulation of isotropic triphasic mixture theory, the MEC behaviors of articular cartilage under an unconfined compression have been studied (74). This in-depth analysis revealed many important new understandings and phenomena observed for articular cartilage. The apparent mechanical properties of such tissues that can be experimentally measured in an unconfined compression experiment are the Young's modulus, Poisson's ratio, and permeability. From Figure 8*a*, we see that the apparent Poisson's ratio [e.g., as measured by an indentation method (24) or by optical method (37)] is always higher than the intrinsic Poisson's ratio of an equivalent uncharged ECM. This is due to the Donnan swelling effect above the hypertonic reference state that is induced by the FCD. Also, from Figure 8*b*, we see that the apparent Young's modulus of a charged tissue is always higher than the intrinsic Young's modulus of an equivalent uncharged ECM. For such materials, the measured apparent Young's modulus is a dependent variable that depends not only on the intrinsic Young's modulus of the solid matrix (an independent variable) but also on the FCD and the intrinsic

Poisson's ratio (an independent variable). Similarly, this dependence holds true for the apparent Poisson's ratio.

Clearly, these new findings are essential in the proper interpretation of all experimental material property measurements for charged-hydrated tissues such as articular cartilage. The FCD generates a variety of electrical phenomena thought to be important in the understanding of the biology of all such tissues for the mechano-signal transduction processes involved in the regulation of cartilage biosynthesis (7, 15, 58, 67, 85–92, 99). The electrical potential inside the tissue comes from two competing sources: diffusion potential (non-uniform distributions of FCD, deformation or natural) and streaming potential (ion convection by interstitial fluid flow). Both potentials depend not only on the values of the FCD and its gradients but also on the intrinsic mechanical properties such as the Young's modulus, Poisson's ratio, and permeability. Within the physiological range of material parameters, the polarity of the potential may be different depending on the values of these intrinsic material properties (Figure 9). For softer tissues (such as those found in osteoarthritis), the diffusion potential tends to dominate, whereas the streaming potential tends to dominate for stiffer tissue (normal cartilage). This phenomenon was first pointed out by Lai and co-workers (62) in two other commonly used experimental configurations, i.e., confined compression and direct permeation (mentioned above).

As discussed with the biphasic theory, the triphasic mixture theory and its finite element formulation also allow a direct examination of inhomogeneity of material properties and FCD on the MEC phenomena inside cartilage tissue and around chondrocytes under loading. Using the new data regarding the inhomogeneous distributions of both fixed charge density and aggregate modulus derived experimentally from combined optical microscopy and mechanical testing (133), the MEC variables inside cartilage have been calculated. The load during the stress-relaxation test is partitioned between the solid and fluid phases of the tissue, manifested as matrix stress and interstitial fluid pressure. In the triphasic model, the fluid pressure derives from both the hydrodynamic fluid pressure and the Donnan osmotic pressure. Accordingly, from Figure 10*a*, the fluid pressure is equal to the osmotic pressure at $t = 0$ and at equilibrium (1200 s) when there is no longer fluid flow or exudation from the tissue. At equilibrium, the measurable load (e.g., calculated total stress) reflects the change in osmotic pressure and solid matrix stress. The electrical potential (Figure 10*b*) in the homogeneous tissue is zero at $t = 0$ and at $t = 1200$ s. This results from the uniform distribution of FCD within the tissue before loading and at equilibrium. In contrast, electrical potential gradients exist in the inhomogeneous FCD case during the entire stress relaxation response. At $t = 0$ and equilibrium, the electrical potential distribution resembles that for the FCD distribution within the inhomogeneous tissue. From Figure 10*b*, there is a sign change in the electrical potential inside the inhomogeneous tissue that is not observed for the homogeneous tissue.

These new multiphasic mixture theories have demonstrated their power in quantification of MEC properties for articular cartilage, as well as prediction of MEC

parameters inside cartilage tissue. With further and careful experimental measurements of those intrinsic MEC material properties for articular cartilage and validation of these theories in comparison with experimental data, there will be an exponential growth of our understanding of cartilage biomechanics, mechano-signal transduction, and cartilage biology.

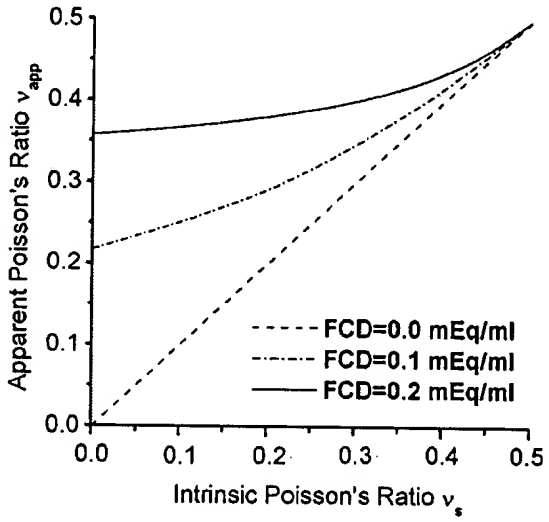

(a)

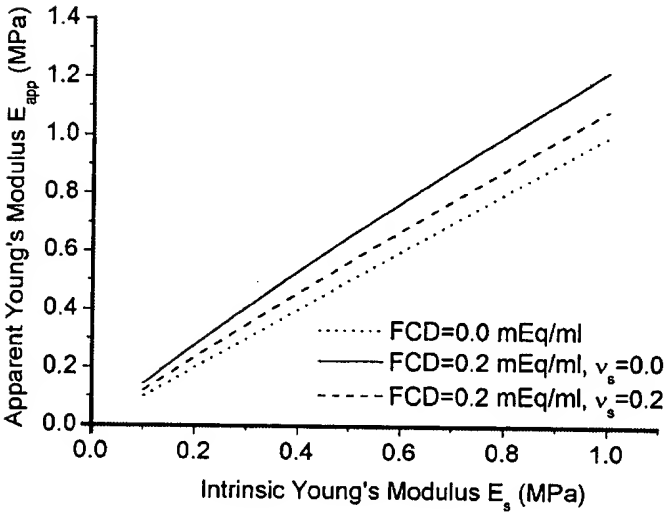

(b)

FUTURE DIRECTIONS IN CARTILAGE MECHANO-ELECTROCHEMISTRY

Within the past decade, significant advances have been made in experimental, theoretical, and biological studies of the basic sciences relating to articular cartilage. New testing techniques have emerged such that articular cartilage can be studied in great detail in terms of its nonlinear and viscoelastic behaviors, depth-dependent inhomogeneity of the MEC properties, and anisotropy characteristics. New advanced theories have been developed that encompass these experimental findings. The knowledge obtained from both fronts, experimental and theoretical, provides enrichment and in-depth understanding of the structure-function relationship in articular cartilage and in all soft-hydrated-charged connective tissues as well. In molecular biology, an explosion of discoveries of cellular and molecular mechanisms in cells, including chondrocytes, has been accumulated. The existing body of literature already indicates the importance of cartilage biomechanics in the generation and maintenance of articular cartilage, as well as regeneration of diseased articular cartilage. Mechano-electrochemical factors already have been linked to the biosynthetic activities and gene expression of chondrocytes. In the next decade of genomic engineering and tissue engineering, cartilage biomechanics will play an even more important role in delineating functions of genes and engineering of cartilage replacements. Such tissue engineering constructs must be able to function in the highly loaded environment of diarthrodial joints for many years. Thus far, success has been elusive and is far from guaranteed in clinical situations.

There is no question that cartilage biomechanics with appropriate, experimentally validated constitutive theory will continue to play crucial and indispensable roles in determining the mechano-signals mechanism for chondrocytes. Important questions remain: What are the crucial and important MEC signals that chondrocytes receive to maintain their normal metabolic functions? What are the

Figure 8 (*a*) The apparent Poisson's ratio of the tissue at equilibrium versus the intrinsic Poisson's ratio of the solid matrix with the FCD as a parameter. The intrinsic shear modulus is fixed as 0.15 MPa. Due to the increased osmotic pressure, the charged tissue has larger lateral expansion than the non-charged tissue whose equilibrium lateral deformation is determined only by the intrinsic Poisson's ratio of the solid matrix. (*b*) The apparent Young's modulus of the charged and uncharged tissues at equilibrium versus the intrinsic Young's modulus of the solid matrix with the same intrinsic Poisson's ratio. For the uncharged case, the apparent Young's modulus is the same as the intrinsic Young's modulus of the solid matrix and is independent of the intrinsic Poisson's ratio of the solid matrix. Due to the increased osmotic pressure, the charged tissue has larger apparent Young's modulus than the uncharged tissue, and the enhancement of the apparent Young's modulus is more remarkable at the low value of the intrinsic Poisson's ratio of the solid matrix, i.e., greater apparent compressibility of the charged matrix.

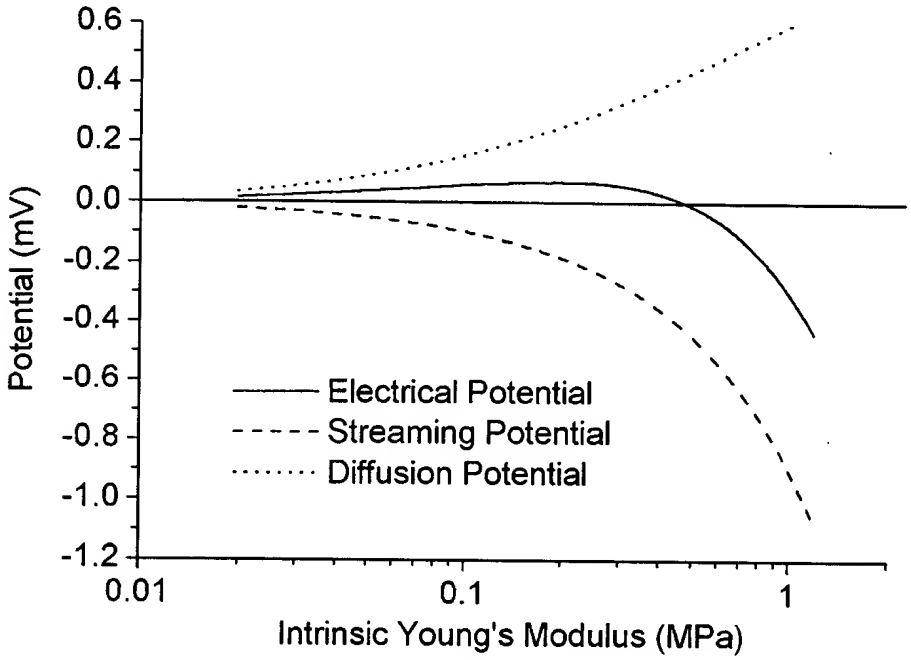

Figure 9 The electrical potential difference inside the tissue and its streaming potential and diffusion potential components calculated at 10 s versus the Young's modulus of the solid matrix with the initial FCD of 0.2 mEq/ml and a Poisson's ratio of 0.2. The electrical potential difference is the electrical potential at the center of the tissue minus the one at the lateral edge inside the tissue. This electrical potential difference is zero when $E_s = 0.46$ MPa.

distributions of these signals (spatial and temporal) in the neighborhood around chondrocytes? How are these MEC signals altered in the diseased state of the tissue such as osteoarthritis? What are the MEC and biochemical clues to ensure successful cartilage tissue engineering? These are exciting frontiers at the intersection of biomechanics, functional genomics, functional tissue engineering, and biology of articular cartilage.

Future experimental studies using new emerging techniques will allow a detailed description of the nonlinear, flow-dependent/flow-independent viscoelastic, anisotropic, and electromechanical behaviors of articular cartilage. These details will be correlated with the spatial and temporal variations in composition,

Figure 10 (*a*) Plot of the spatial distribution and temporal development of fluid pressure for the homogeneous and inhomogeneous tissue subjected to stress relaxation in confined compression. (*b*) Plot of the spatial distribution and temporal development of electrical potential for the homogeneous and inhomogeneous tissue subjected to stress relaxation in confined compression.

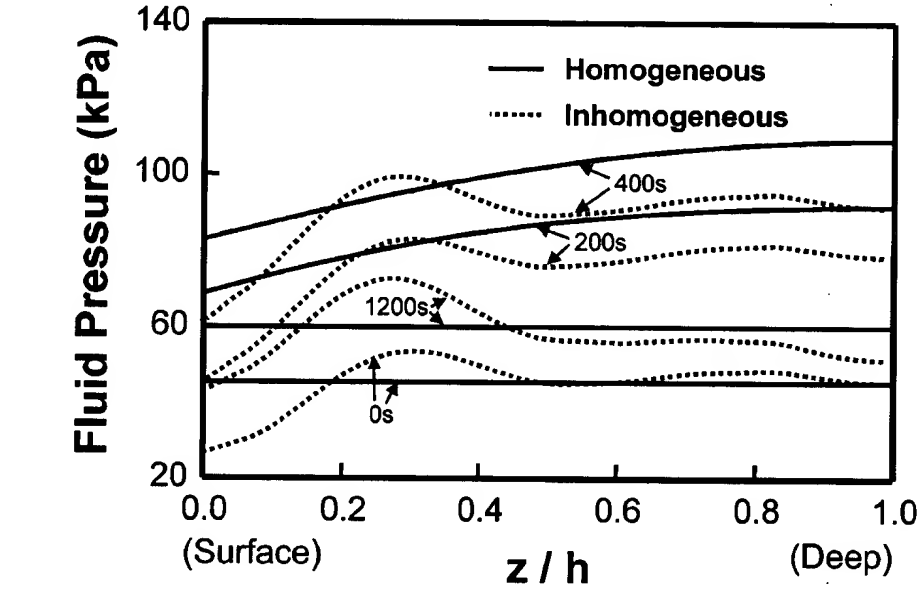
Fluid Pressure (kPa)
140
100
60
20
Homogeneous
Inhomogeneous
400s
200s
1200s
0s
0.0
0.2
0.4
0.6
0.8
1.0
(Surface)
z / h
(Deep)

(a)

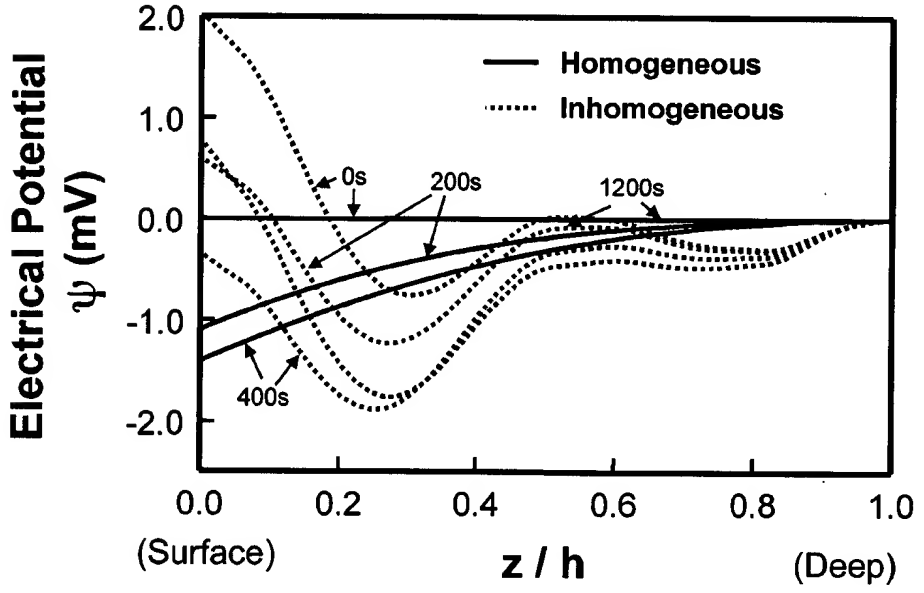
Electrical Potential
ψ (mV)
2.0
1.0
0.0
-1.0
-2.0
Homogeneous
Inhomogeneous
0s
200s
1200s
400s
0.0
0.2
0.4
0.6
0.8
1.0
(Surface)
z / h
(Deep)

(b)

structure, and function of articular cartilage, and such fundamental experimental findings will be incorporated in the refined constitutive theories of articular cartilage, and functional cartilage tissue engineering (99, 134–136). The MEC parameters can and will be calculated down to the cellular and molecular level (i.e., molecular biomechanics of cartilage structure and function) and integrated into the biochemical and biophysical pathways of cellular and molecular regulation of chondrocyte functions. The practical and clinical applications of these findings and theories will play more crucial roles in surgical planning and outcome assessments of joint surgeries with improved of computational models.

ACKNOWLEDGMENTS

This work was sponsored in part by grants from the National Institutes of Health (AR41913, AR38733 and AR45832) and the Whitaker Foundation (97-0086).

The *Annual Review of Biomedical Engineering* is online at http://bioeng.annualreviews.org

LITERATURE CITED

1. Mow VC, Ratcliffe A. 1997. Structure and function of articular cartilage and meniscus. In *Basic Orthopaedic Biomechanics.* ed. VC Mow, WC Hayes, pp. 113–77. Philadelphia: Lippincott-Raven. 2nd ed.

1a. Mow VC, Hayes WC, eds. 1997. *Basic Orthopaedic Biomechanics*. 2nd ed. Philadelphia: Lippincott-Raven

2. Mow VC, Ateshian GA, Spilker RL. 1993. Biomechanics of diarthrodial joints: a review of twenty years of progress. *J. Biomech. Eng.* 115:460–67

3. Mow VC, Ateshian GA. 1997. Lubrication and wear of diarthrodial joints. See Ref. 1a, pp. 275–315

4. Akizuki S, Mow VC, Muller F, Pita JC, Howell DS. 1987. Tensile properties of human knee joint cartilage. II. Correlations between weight bearing and tissue pathology and the kinetics of swelling. *J. Orthop. Res.* 5:173–86

5. Armstrong CG, Mow VC. 1982. Variations in the intrinsic mechanical properties of human articular cartilage with age, degeneration, and water content. *J. Bone Joint Surg. Am. Vol.* 64:88–94

6. Maroudas A. 1979. Physicochemical properties of articular cartilage. In *Adult Articular Cartilage.* ed. MAR Freeman, pp. 215–323. Kent, UK: Pitman Med. 2nd ed.

7. Mankin HJ, Mow VC, Buckwalter JA. 2000. Articular cartilage repair and osteoarthritis. In *Orthopaedic Basic Science: Biology and Biomechanics of the Musculoskeletal System.* ed. JA Buckwalter, TA Einhorn, SR Simon. Rosemont, IL: Am. Acad. Orthop. Surg.

8. Eyre DR. 1991. The collagens of articular cartilage. *Sem. Arthritis Rheumatism* 21:2–11

9. Clark JM, Simonian PT. 1997. Scanning electron microscopy of "fibrillated" and "malacic" human articular cartilage: technical considerations. *Microsc. Res. Tech.* 37:299–313

10. Setton LA, Zhu W, Mow VC. 1993. The biphasic poroviscoelastic behavior of articular cartilage: role of the surface zone in governing the compressive behavior. *J. Biomech.* 26:581–92

11. Guilak F, Ratcliffe A, Lane N, Rosenwasser MP, Mow VC. 1994. Mechanical

and biochemical changes in the superficial zone of articular cartilage in canine experimental osteoarthritis. *J. Orthop. Res.* 12:474–84

12. Jeffrey JE, Thomson LA, Aspden RM. 1997. Matrix loss and synthesis following a single impact load on articular cartilage in vitro. *Biochim. Biophys. Acta* 1334:223–32
13. Clarke IC. 1971. Articular cartilage: a review and scanning electron microscope study. 1. The interterritorial fibrillar architecture. *J. Bone Joint Surg. Br.* 53: 732–50
14. Clark JM. 1991. Variation of collagen fiber alignment in a joint surface: a scanning electron microscope study of the tibial plateau in dog, rabbit, and man. *J. Orthop. Res.* 9:246–57
15. Muir H. 1983. Proteoglycans as organizers of the intercellular matrix. *Biochem. Soc. Trans.* 11:613–22
16. Hardingham TE, Fosang AJ. 1992. Proteoglycans: many forms and many functions. *FASEB J.* 6:861–70
17. Maroudas A. 1968. Physicochemical properties of cartilage in the light of ion exchange theory. *Biophys. J.* 8:575–95
18. Muir H, Bullough P, Maroudas A. 1970. The distribution of collagen in human articular cartilage with some of its physiological implications. *J. Bone Joint Surg. Br.* 52:554–63
19. Broom ND, Marra DL. 1986. Ultrastructural evidence for fibril-to-fibril associations in articular cartilage and their functional implication. *J. Anat.* 146:185–200
20. Redler I, Mow VC, Zimny ML, Mansell J. 1975. The ultrastructure and biomechanical significance of the tidemark of articular cartilage. *Clin. Orthop. Rel. Res.* 112: 357–62
21. Setton LA, Tohyama H, Mow VC. 1998. Swelling and curling behaviors of articular cartilage. *J. Biomech. Eng.* 120:355–61
22. Mow VC, Kuei SC, Lai WM, Armstrong CG. 1980. Biphasic creep and stress relaxation of articular cartilage in compression: theory and experiments. *J. Biomech. Eng.* 102:73–84
23. Lai WM, Mow VC. 1980. Drag-induced compression of articular cartilage during a permeation experiment. *Biorheology* 17:111–23
24. Mow VC, Gibbs MC, Lai WM, Zhu WB, Athanasiou KA. 1989. Biphasic indentation of articular cartilage. II. A numerical algorithm and an experimental study. *J. Biomech.* 22:853–61
25. Elmore SM, Sokoloff L, Norris G, Carmeci P. 1962. Nature of "imperfect" elasticity of articular cartilage. *J. Appl. Physiol.* 18:393–96
26. Mow VC, Ratcliffe A, Poole AR. 1992. Cartilage and diarthrodial joints as paradigms for hierarchical materials and structures. *Biomaterials* 13:67–97
27. Gu WY, Mao XG, Rawlins BA, Iatridis JC, Foster RJ, et al. 1999. Streaming potential of human lumbar annulus fibrosus is anisotropic and affected by disc degeneration. *J. Biomech.* 32:1177–82
28. Maroudas A. 1976. Transport of solutes through cartilage: permeability to large molecules. *J. Anat.* 122:335–47
29. Mow VC, Holmes MH, Lai WM. 1984. Fluid transport and mechanical properties of articular cartilage: a review. *J. Biomech.* 17:377–94
30. Gu WY, Lai WM, Mow VC. 1993. Transport of fluid and ions through a porous-permeable charged-hydrated tissue, and streaming potential data on normal bovine articular cartilage. *J. Biomech.* 26:709–23
31. Gu WY, Lai WM, Mow VC. 1998. A mixture theory for charged-hydrated soft tissues containing multi-electrolytes: passive transport and swelling behaviors. *J. Biomech. Eng.* 120:169–80
32. Holmes MH, Lai WM, Mow VC. 1985. Singular perturbation analysis of the nonlinear, flow-dependent compressive stress relaxation behavior of articular cartilage. *J. Biomech. Eng.* 107:206–18

33. Holmes MH, Mow VC. 1990. The nonlinear characteristics of soft gels and hydrated connective tissues in ultrafiltration. *J. Biomech.* 23:1145–56
34. Soltz MA, Ateshian GA. 1998. Experimental verification and theoretical prediction of cartilage interstitial fluid pressurization at an impermeable contact interface in confined compression. *J. Biomech.* 31:927–34
35. Soltz MA, Ateshian GA. 2000. Interstitial fluid pressurization during confined compression cyclical loading of articular cartilage. *Ann. Biomed. Eng.* 28:150–59
36. Armstrong CG, Lai WM, Mow VC. 1984. An analysis of the unconfined compression of articular cartilage. *J. Biomech. Eng.* 106:165–73
37. Jurvelin JS, Buschmann MD, Hunziker EB. 1997. Optical and mechanical determination of Poisson's ratio of adult bovine humeral articular cartilage. *J. Biomech.* 30:235–41
38. Athanasiou KA, Rosenwasser MP, Buckwalter JA, Malinin TI, Mow VC. 1991. Interspecies comparisons of in situ intrinsic mechanical properties of distal femoral cartilage. *J. Orthop. Res.* 9:330–40
39. Lyyra-Laitinen T, Niinimaki M, Toyras J, Lindgren R, Kiviranta I, et al. 1999. Optimization of the arthroscopic indentation instrument for the measurement of thin cartilage stiffness. *Phys. Med. Biol.* 44:2511–24
40. Lyyra T, Kiviranta I, Vaatainen U, Helminen HJ, Jurvelin JS. 1999. In vivo characterization of indentation stiffness of articular cartilage in the normal human knee. *J. Biomed. Mater. Res.* 48:482–87
41. Froimson MI, Ratcliffe A, Gardner TR, Mow VC. 1997. Differences in patellofemoral joint cartilage material properties and their significance to the etiology of cartilage surface fibrillation. *Osteoarthritis Cartilage* 5:377–86
42. Athanasiou KA, Agarwal A, Dzida FJ. 1994. Comparative study of the intrinsic mechanical properties of the human acetabular and femoral head cartilage. *J. Orthop. Res.* 12:340–49
43. Kempson GE. 1979. Mechanical properties of articular cartilage. In *Adult Articular Cartilage*, ed. MAR Freeman, pp. 334–414. Kent, UK: Pitman Med. 2nd ed.
44. Woo SY, Akeson WH, Jemmott GF. 1976. Measurements of non-homogeneous directional mechanical properties of articular cartilage in tension. *J. Biomech.* 9:785–91
45. Roth V, Mow VC. 1980. The intrinsic tensile behavior of the matrix of bovine articular cartilage and its variation with age. *J. Bone Joint Surg. Am. Vol.* 62:1102–17
46. Akizuki S, Mow VC, Muller F, Pita JC, Howell DS, et al. 1986. Tensile properties of human knee joint cartilage. I. Influence of ionic conditions, weight bearing, and fibrillation on the tensile modulus. *J. Orthop. Res.* 4:379–92
47. Kempson GE, Muir H, Pollard C, Tuke M. 1973. The tensile properties of the cartilage of human femoral condyles related to the content of collagen and glycosaminoglycans. *Biochim. Biophys. Acta* 297:456–72
48. Schmidt MB, Mow VC, Chun LE, Eyre DR. 1990. Effects of proteoglycan extraction on the tensile behavior of articular cartilage. *J. Orthop. Res.* 8:353–63
49. Kempson GE. 1982. Relationship between the tensile properties of articular cartilage from the human knee and age. *Ann. Rheumatic Dis.* 41:508–11
50. Kempson GE. 1991. Age-related changes in the tensile properties of human articular cartilage: a comparative study between the femoral head of the hip joint and the talus of the ankle joint. *Biochim. Biophys. Acta* 1075:223–30
51. Huang C-H, Mow VC, Ateshian GA. 2001. The role of flow-independent viscoelasticity in the biphasic tensile and compressive responses of articular cartilage. *J. Biomech. Eng.* 123:410–17
52. Huang C-Y, Soltz MA, Kopacz M, Mow VC, Ateshian GA. 2002. Experimental

verification of the role of intrinsic matrix viscoelasticity and tension-compression nonlinearity in the biphasic responses of cartilage in unconfined compression. *J. Biomech. Eng.* In press
53. Curnier A, He QC, Zysset PK. 1995. Conewise linear elastic materials. *J. Elast.* 37:1–38
54. Soltz MA, Ateshian GA. 2000. A conewise linear elasticity mixture model for the analysis of tension-compression nonlinearity in articular cartilage. *J. Biomech. Eng.* 122:576–86
55. Myers ER, Lai WM, Mow VC. 1984. A continuum theory and an experiment for the ion-induced swelling behavior of articular cartilage. *J. Biomech. Eng.* 106: 151–58
56. LeRoux MA, Arokoski J, Vail TP, Guilak F, Hyttinen MM, et al. 2000. Simultaneous changes in the mechanical properties, quantitative collagen organization, and proteoglycan concentration of articular cartilage following canine meniscectomy. *J. Orthop. Res.* 18:383–92
57. Wang C-B, Chahine NO, Hung CT, Ateshian GA. 2002. Optical determination of anisotropic material properties of bovine articular cartilage in compression. *J. Biomech.* In press
58. Maroudas A, Ziv I, Weisman N, Venn M. 1985. Studies of hydration and swelling pressure in normal and osteoarthritic cartilage. *Biorheology* 22:159–69
59. Maroudas A, Wachtel E, Grushko G, Katz EP, Weinberg P. 1991. The effect of osmotic and mechanical pressures on water partitioning in articular cartilage. *Biochim. Biophys. Acta* 1073:285–94
60. Lai WM, Hou JS, Mow VC. 1991. A triphasic theory for the swelling and deformation behaviors of articular cartilage. *J. Biomech. Eng.* 113:245–58
61. Mow VC, Ateshian GA, Lai WM, Gu WY. 1998. Effects of fixed charges on the stress relaxation behavior of hydrated soft tissue in a confined compression problem. *Int. J. Struct. Solids* 35:4945–62
62. Lai WM, Mow VC, Sun DD, Ateshian GA. 2000. On the electric potentials inside a charged soft hydrated biological tissue: streaming potential versus diffusion potential. *J. Biomech. Eng.* 122:336–46
63. Donnan FG. 1924. The theory of membrane equilibria. *Chem. Rev.* 1:73–90
64. Maroudas A. 1976. Balance between swelling pressure and collagen tension in normal and degenerate cartilage. *Nature* 260:1089–95
65. Maroudas A, Venn M. 1977. Chemical composition and swelling of normal and osteoarthrotic femoral head cartilage. II. Swelling. *Ann. Rheumatic Dis.* 36:399–406
66. Grodzinsky AJ, Roth V, Myers E, Grossman WD, Mow VC. 1981. The significance of electromechanical and osmotic forces in the nonequilibrium swelling behavior of articular cartilage in tension. *J. Biomech. Eng.* 103:221–31
67. Frank EH, Grodzinsky AJ. 1987. Cartilage electromechanics. II. A continuum model of cartilage electrokinetics and correlation with experiments. *J. Biomech.* 20:629–39
68. Kim YJ, Bonassar LJ, Grodzinsky AJ. 1995. The role of cartilage streaming potential, fluid flow and pressure in the stimulation of chondrocyte biosynthesis during dynamic compression. *J. Biomech.* 28:1055–66
69. Chen AC, Bae WC, Schinagl RM, Sah RL. 2001. Depth- and strain-dependent mechanical and electromechanical properties of full-thickness bovine articular cartilage in confined compression. *J. Biomech.* 34:1–12
70. Chen AC, Nguyen TT, Sah RL. 1997. Streaming potentials during the confined compression creep test of normal and proteoglycan-depleted cartilage. *Ann. Biomed. Eng.* 25:269–77
71. Huyghe JM, Janssen JD. 1997. Quadriphasic mechanics of swelling incompressible porous media. *Int. J. Eng. Sci.* 35: 793–802

72. Frijns AJH, Huyghe JM, Janssen JD. 1997. A validation of the quadriphaisc mixture theory for intervertebral disc tissue. *Int. J. Eng. Sci.* 35:1419–29
73. Sun DN, Gu WY, Guo XE, Lai WM, Mow VC. 1999. A mixed finite element formulation of triphasic mechano-electrochemical theory for charged, hydrated biological soft tissues. *Int. J. Num. Methods Eng.* 45:1375–402
74. Sun DN, Guo XE, Likhitpanichkul M, Lai WM, Mow VC. 2002. The influence of the fixed negative charges on mechanical and electrical behaviors in articular cartilage. *J. Biomech. Eng.* In review
75. Chen SS, Falcovitz YH, Schneiderman R, Maroudas A, Sah RL. 2001. Depth-dependent compressive properties of normal aged human femoral head articular cartilage: relationship to fixed charge density. *Osteoarthritis Cartilage* 9:561–69
76. Mow VC, Wang CC, Hung CT. 1999. The extracellular matrix, interstitial fluid and ions as a mechanical signal transducer in articular cartilage. *Osteoarthritis Cartilage* 7:41–58
77. Lai WM, Sun DN, Ateshian GA, Guo XE, Mow VC. 2000. *Effects of inhomogeneous fixed charge density on the electrical signals for chondrocytes in cartilage.* Proc. ASME Symp. Mechanics in Biology, Orlando, FL, AMD-242/BED- 46:201–13
78. Guilak F, Mow VC. 2000. The mechanical environment of the chondrocyte: a biphasic finite element model of cell-matrix interactions in articular cartilage. *J. Biomech.* 33:1663–73
79. Guilak F, Tedrow JR, Burgkart R. 2000. Viscoelastic properties of cell nucleus. *Biochem. Biophys. Res. Commun.* 269:781–86
80. Stockwell RA. 1979. *Biology of Cartilage Cells.* Cambridge, UK: Cambridge Univ. Press
81. Schinagl RM, Ting MK, Price JH, Sah RL. 1996. Video microscopy to quantitate the inhomogeneous equilibrium strain within articular cartilage during confined compression. *Ann. Biomed. Eng.* 24:500–12
82. Schinagl RM, Gurskis D, Chen AC, Sah RL. 1997. Depth-dependent confined compression modulus of full-thickness bovine articular cartilage. *J. Orthop. Res.* 15:499–506
83. Wang CC, Hung CT, Mow VC. 2001. An analysis of the effects of depth-dependent aggregate modulus on articular cartilage stress-relaxation behavior in compression. *J. Biomech.* 34:75–84
84. Wang C-B, Guo XE, Sun D-N, Mow VC, Ateshian GA, et al. 2002. The functional environment of chondrocytes within cartilage subjected to compressive loading: a theoretical and experimental approach. *Biorheology.* In press
85. Schneiderman R, Keret D, Maroudas A. 1986. Effects of mechanical and osmotic pressure on the rate of glycosaminoglycan synthesis in the human adult femoral head cartilage: an in vitro study. *J. Orthop. Res.* 4:393–408
86. Mow VC, Bachrach NM, Setton LA, Guilak F. 1994. Stress, strain, pressure, and flow fields in articular cartilage and chondrocytes. In *Cell Mechanics and Cellular Engineering*, ed. VC Mow, F Guilak, R Tran-Son-Tay, RM Hochmuth, pp. 147–71. New York: Springer-Verlag
87. Kim YJ, Sah RL, Grodzinsky AJ, Plaas AH, Sandy JD. 1994. Mechanical regulation of cartilage biosynthetic behavior: physical stimuli. *Arch. Biochem. Biophys.* 311:1–12
88. Guilak F, Ratcliffe A, Mow VC. 1995. Chondrocyte deformation and local tissue strain in articular cartilage: a confocal microscopy study. *J. Orthop. Res.* 13:410–21
89. Bachrach NM, Valhmu WB, Stazzone E, Ratcliffe A, Lai WM, et al. 1995. Changes in proteoglycan synthesis of chondrocytes in articular cartilage are associated with the time-dependent changes in their mechanical environment. *J. Biomech.* 28:1561–69
90. Kim YJ, Grodzinsky AJ, Plaas AH. 1996.

Compression of cartilage results in differential effects on biosynthetic pathways for aggrecan, link protein, and hyaluronan. *Arch. Biochem. Biophys.* 328:331–40
91. Guilak F, Sah RL, Setton LA. 1997. Physical regulation of cartilage metabolism, See Ref. 1a, pp. 170–207
92. Valhmu WB, Stazzone EJ, Bachrach NM, Saed-Nejad F, Fischer SG, et al. 1998. Load-controlled compression of articular cartilage induces a transient stimulation of aggrecan gene expression. *Arch. Biochem. Biophys.* 353:29–36
93. Brandt KD, Braunstein EM, Visco DM, O'Connor B, Heck D, et al. 1991. Anterior (cranial) cruciate ligament transection in the dog: a bona fide model of osteoarthritis, not merely of cartilage injury and repair. *J. Rheumatol.* 18:436–46
94. Setton LA, Mow VC, Muller FJ, Pita JC, Howell DS. 1997. Mechanical behavior and biochemical composition of canine knee cartilage following periods of joint disuse and disuse with remobilization. *Osteoarthritis Cartilage* 5:1–16
95. Hodge WA, Fijan RS, Carlson KL, Burgess RG, Harris WH, et al. 1986. Contact pressures in the human hip joint measured in vivo. *Proc. Natl. Acad. Sci. USA* 83:2879–83
96. Ateshian GA, Wang H. 1997. Rolling resistance of articular cartilage due to interstitial fluid flow. *Proc. Inst. Mech. Eng. H* 211:419–24
97. Ateshian GA. 1997. A theoretical formulation for boundary friction in articular cartilage. *J. Biomech. Eng.* 119:81–86
98. Dowson D. 1990. Bio-tribology of natural and replacement synovial joint. In *Biomechanics of Diarthrodial Joints*, ed. VC Mow, A Ratcliffe, SL-Y Woo, pp. 305–45. New York: Springer-Verlag
99. Butler DL, Goldstein SA, Guilak F. 2000. Functional tissue engineering: the role of biomechanics. *J. Biomech. Eng.* 122:570–75
100. Donzelli PS, Spilker RL, Ateshian GA, Mow VC. 1999. Contact analysis of biphasic transversely isotropic cartilage layers and correlations with tissue failure. *J. Biomech.* 32:1037–47
101. DiSilvestro MR, Zhu Q, Wong M, Jurvelin JS, Suh JK. 2001. Biphasic poroviscoelastic simulation of the unconfined compression of articular cartilage. I. Simultaneous prediction of reaction force and lateral displacement. *J. Biomech. Eng.* 123:191–97
102. DiSilvestro MR, Zhu Q, Suh JK. 2001. Biphasic poroviscoelastic simulation of the unconfined compression of articular cartilage. II. Effect of variable strain rates. *J. Biomech. Eng.* 123:198–200
103. Ateshian GA, Soslowsky LJ, Mow VC. 1991. Quantitation of articular surface topography and cartilage thickness in knee joints using stereophotogrammetry. *J. Biomech.* 24:761–76
104. Ateshian GA, Soslowsky LJ. 1997. Quantitative anatomy of diarthrodial joint articular layers. See Ref. 1a, pp. 253–73
105. Cohen ZA, McCarthy DM, Kwak SD, Legrand P, Fogarasi F, et al. 1999. Knee cartilage topography, thickness, and contact areas from MRI: in-vitro calibration and in-vivo measurements. *Osteoarthritis Cartilage* 7:95–109
106. Andriacchi TP. 1997. Musculoskeletal dynamics, locomotion, and clinical applications. See Ref. 1a, pp. 37–68
107. Schwartz MH, Leo PH, Lewis JL. 1994. A microstructural model for the elastic response of articular cartilage. *J. Biomech.* 27:865–73
108. Wren TA, Carter DR. 1998. A microstructural model for the tensile constitutive and failure behavior of soft skeletal connective tissues. *J. Biomech. Eng.* 120:55–61
109. Bursac P, McGrath CV, Eisenberg SR, Stamenovic D. 2000. A microstructural model of elastostatic properties of articular cartilage in confined compression. *J. Biomech. Eng.* 122:347–53
110. Ingber DE. 1991. Integrins as mechanochemical transducers. *Curr. Opin. Cell Biol.* 3:841–48

111. Ahmed AM, Burke DL, Yu A. 1983. In vitro measurement of static pressure distribution in synovial joints. II. Retropatellar surface. *J. Biomech. Eng.* 105:226–36
112. Ateshian GA, Kwak SD, Soslowsky LJ, Mow VC. 1994. A stereophotogrammetric method for determining in situ contact areas in diarthrodial joints, and a comparison with other methods. *J. Biomech.* 27:111–24
113. Ateshian GA, Lai WM, Zhu WB, Mow VC. 1994. An asymptotic solution for the contact of two biphasic cartilage layers. *J. Biomech.* 27:1347–60
114. Wu JZ, Herzog W. 2000. Finite element simulation of location- and time-dependent mechanical behavior of chondrocytes in unconfined compression tests. *Ann. Biomed. Eng.* 28:318–30
115. Spilker RL, Suh JK, Mow VC. 1990. Effects of friction on the unconfined compressive response of articular cartilage: a finite element analysis. *J. Biomech. Eng.* 112:138–46
116. Suh JK, Spilker RL, Holmes MH. 1991. A penalty finite element analysis for nonlinear mechanics of biphasic hydrated soft tissue under large deformation. *Int. J. Num. Methods Eng.* 32:1411–39
117. Spilker RL, Suh JK, Mow VC. 1992. A finite element analysis of the indentation stress-relaxation response of linear biphasic articular cartilage. *J. Biomech. Eng.* 114:191–201
118. Suh JK, Bai S. 1998. Finite element formulation of biphasic poroviscoelastic model for articular cartilage. *J. Biomech. Eng.* 120:195–201
119. Wu JZ, Herzog W, Epstein M. 1998. Evaluation of the finite element software ABAQUS for biomechanical modelling of biphasic tissues. *J. Biomech.* 31:165–69
120. Cohen B, Lai WM, Mow VC. 1998. A transversely isotropic biphasic model for unconfined compression of growth plate and chondroepiphysis. *J. Biomech. Eng.* 120:491–96
121. de Boer R. 2000. Contemporary progress in porous media theory. *Appl. Mech. Rev.* 53:323–69
122. Ehlers W, Bernd M. 2001. A linear viscoelastic biphasic model for soft tissues based on the theory of porous media. *J. Biomech. Eng.* 123:418–24
123. Mak AF. 1986. The apparent viscoelastic behavior of articular cartilage. The contributions from the intrinsic viscoelasticity and interstitial fluid flow. *J. Biomech. Eng.* 108:123–30
124. Soulhat J, Buschmann MD, Shirazi-Adl A. 1999. A fibril-network-reinforced biphasic model of cartilage in unconfined compression. *J. Biomech. Eng.* 121:340–47
125. Hayes WC, Bodine AJ. 1978. Flow-independent viscoelastic properties of articular cartilage matrix. *J. Biomech.* 11: 407–19
126. Zhu W, Mow VC, Koob TJ, Eyre DR. 1993. Viscoelastic shear properties of articular cartilage and the effects of glycosidase treatments. *J. Orthop. Res.* 11:771–81
127. Poole AC. 1997. Articular cartilage chondrons: form, function and failure. *J. Anat.* 191:1–13
128. Grodzinsky AJ, Lipshitz H, Glimcher MJ. 1978. Electromechanical properties of articular cartilage during compression and stress relaxation. *Nature* 275:448–50
129. Basser PJ, Grodzinsky AJ. 1993. The Donnan model derived from microstructure. *Biophys. Chem.* 46:57–68
130. Buschmann MD, Grodzinsky AJ. 1995. A molecular model of proteoglycan-associated electrostatic forces in cartilage mechanics. *J. Biomech. Eng.* 117:179–92
131. Frank EH, Grodzinsky AJ. 1987. Cartilage electromechanics. I. Electrokinetic transduction and the effects of electrolyte pH and ionic strength. *J. Biomech.* 20: 615–27

132. Katchalsky A, Curran PF. 1975. *Non-Equilibrium Thermodynamics in Biophysics*, Chpt. 11, 12. Cambridge, MA: Harvard Univ. Press
133. Wang C-BC, Guo XE, Deng JJ, Mow VC, Ateshian GA, et al. 2001. *A novel non-invasive technique for determining distribution of fixed charge density within articular cartilage*. Proc. 47th Ann. Meet. Orthopaedic Res. Soc. Orlando, FL, 26: 129
134. Freed LE, Martin I, Vunjak-Novakovic G. 1999. Frontiers in tissue engineering. In vitro modulation of chondrogenesis. *Clin. Orthop. Rel. Res.* 367:S46–58
135. Schaefer D, Martin I, Shastri P, Padera RF, Langer R, et al. 2000. In vitro generation of osteochondral composites. *Biomaterials* 21:2599–606
136. Martin I, Obradovic B, Treppo S, Grodzinsky AJ, Langer R, et al. 2000. Modulation of the mechanical properties of tissue engineered cartilage. *Biorheology* 37:141–47

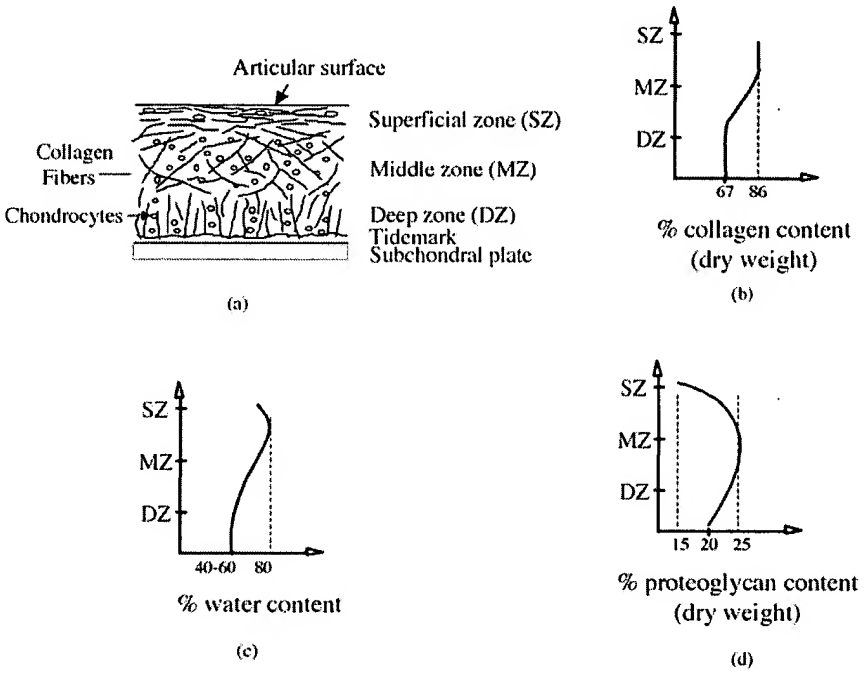

Figure 1 (*a*) A schematic representation of collagen ultrastructural arrangements in the articular cartilage. The superficial tangential zone is a region of densely packed collagen sheets with fibers woven randomly in the plane. In the middle zone, the collagen fibers are more loosely packed and are randomly orientated. In the deep zone, the collagen fibers anatomose forming larger bundles prior to insertion into the calcified zone across the tidemark. (*b*) The distribution of collagen per dry weight as a function of depth from the articular surface. Note the concentration of collagen throughout the depth reflects the collagen ultrastructural organization. (*c*) The distribution of water content [(total weight minus dry weight)/total weight] as a function of depth from the articular surface. (*d*) The distribution of proteoglycan content per dry weight as a function of depth from the articular surface.

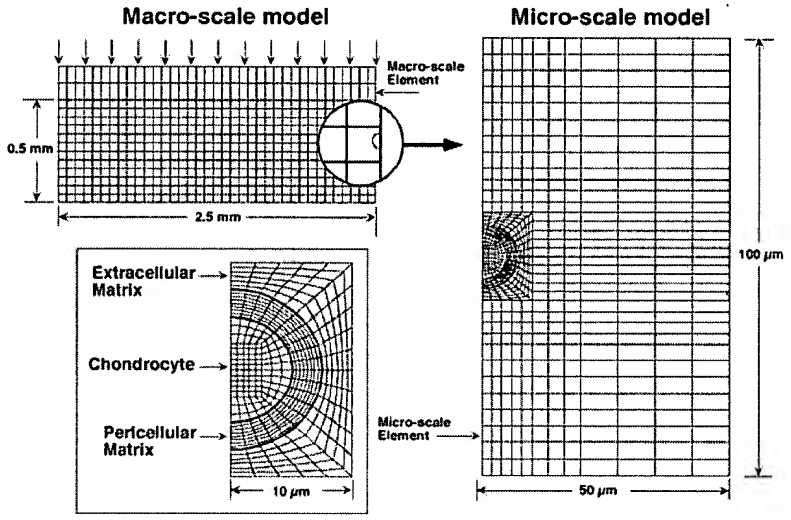

(a)

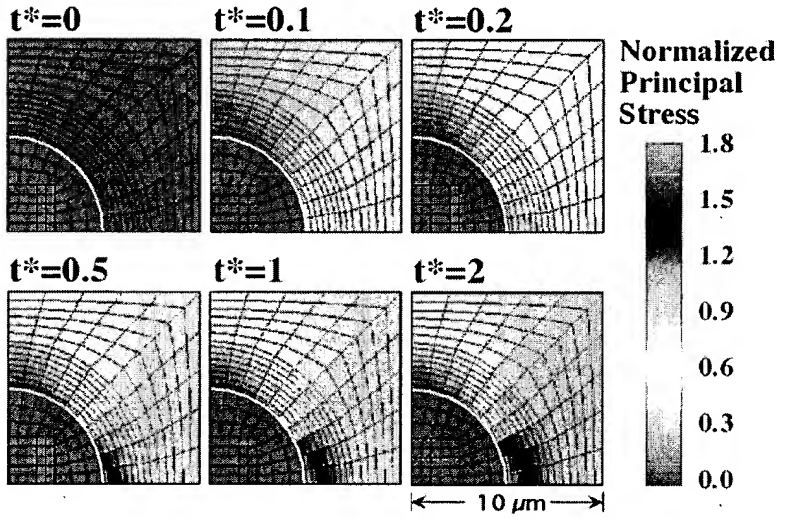

(b)

Figure 7 (*a*) A schematic of a two-scale biphasic finite element model of chondrocyte-matrix interactions under compression. (*b*) The results of normalized principal stress contour plots indicate that the mechanical environment in chondrocyte is both spatial and time-dependent.

EXHIBIT D

Journal of Cell Science 108, 1497-1508 (1995)
Printed in Great Britain © The Company of Biologists Limited 1995

Mechanical compression modulates matrix biosynthesis in chondrocyte/agarose culture

Michael D. Buschmann[1,2], Yehezkiel A. Gluzband[1], Alan J. Grodzinsky[1,*] and Ernst B. Hunziker[2]

[1]Continuum Electromechanics Group, Laboratory for Electromagnetic and Electronic Systems, Department of Electrical Engineering and Computer Science, Massachusetts Institute of Technology, Cambridge, MA 02139
[2]M. E. Müller-Institut für Biomechanik, Universität Bern, Bern, Switzerland

*Author for correspondence

SUMMARY

This study focuses on the effect of static and dynamic mechanical compression on the biosynthetic activity of chondrocytes cultured within agarose gel. Chondrocyte/agarose disks (3 mm diameter) were placed between impermeable platens and subjected to uniaxial unconfined compression at various times in culture (2-43 days). [^{35}S]sulfate and [^{3}H]proline radiolabel incorporation were used as measures of proteoglycan and protein synthesis, respectively. Graded levels of static compression (up to 50%) produced little or no change in biosynthesis at very early times, but resulted in significant decreases in synthesis with increasing compression amplitude at later times in culture; the latter observation was qualitatively similar to that seen in intact cartilage explants. Dynamic compression of ~3% dynamic strain amplitude (≃30 μm displacement amplitude) at 0.01-1.0 Hz, superimposed on a static offset compression, stimulated radiolabel incorporation by an amount that increased with time in culture prior to loading as more matrix was deposited around and near the cells. This stimulation was also similar to that observed in cartilage explants. The presence of greater matrix content at later times in culture also created differences in biosynthetic response at the center versus near the periphery of the 3 mm chondrocyte/agarose disks. The fact that chondrocyte response to static compression was significantly affected by the presence or absence of matrix, as were the physical properties of the disks, suggested that cell-matrix interactions (e.g. mechanical and/or receptor mediated) and extracellular physicochemical effects (increased [Na^+], reduced pH) may be more important than matrix-independent cell deformation and transport limitations in determining the biosynthetic response to static compression. For dynamic compression, fluid flow, streaming potentials, and cell-matrix interactions appeared to be more significant as stimuli than the small increase in fluid pressure, altered molecular transport, and matrix-independent cell deformation. The qualitative similarity in the biosynthetic response to mechanical compression of chondrocytes cultured in agarose gel and chondrocytes in intact cartilage further indicates that gel culture preserves certain physiological features of chondrocyte behavior and can be used to investigate chondrocyte response to physical and chemical stimuli in a controlled manner.

Key words: cartilage, chondrocyte, proteoglycan, matrix biomechanics, agarose, stress-mechanical

INTRODUCTION

Articular cartilage is the dense connective tissue that functions as a bearing material in synovial joints. Adult articular cartilage is avascular, aneural and alymphatic; cell nutrition is derived primarily from the synovial fluid (Mankin and Brandt, 1984). Nutrition in immature cartilage is aided by the presence of vascular canals. The chondrocytes are responsible for the synthesis, maintenance, and gradual turnover of an extracellular matrix (ECM) composed principally of a hydrated collagen fibril network enmeshed in a gel of highly charged proteoglycan (PG) molecules. The composition and architecture of the matrix (Maroudas, 1979) and the tissue's high water content (70-80% of wet weight) enable cartilage to withstand complex compressive, tensile and shear forces in joints (Hodge et al., 1986; Mow et al., 1984).

Cartilage extracellular matrix can remodel to meet the functional demands of loading. For example, repulsive electrostatic (osmotic) interactions between the proteoglycan constituents of the ECM enable cartilage to resist compressive loads (Buschmann and Grodzinsky, 1995; Buschmann, 1992; Grodzinsky, 1983; Maroudas, 1979). Animal studies have shown that PG content is higher in cartilage that is habitually loaded (Caterson and Lowther, 1978; Kiviranta et al., 1988; Salter et al., 1980), while immobilization of joints leads to a decrease in PG synthesis and total PG content (Akeson et al., 1973; Kiviranta et al., 1987; Olah and Kostenszky, 1972; Palmoski et al., 1979). There do appear to be limits in the ability of chondrocytes to respond to altered functional demands. Increasing intensity of normal usage (without experimental modification of normal joint anatomy) can eventually result in a reduction in PG content (Arokoski et al., 1993; Jurvelin et al.,

1990; Kiviranta et al., 1992). Animal models of osteoarthritis in which an abrupt change in joint motion is surgically introduced lead to profound attempts at adaptation but eventually result in cartilage deterioration and malfunction (Inerot et al., 1991). The mechanisms that mediate the biological response to mechanical loads in cartilage are not well understood.

Biosynthesis, metabolism, and turnover of cartilage matrix components have been studied extensively in vivo and using cell and tissue culture models (Kuettner et al., 1986). Recent in vitro studies have shown that mechanical loads can also induce metabolic responses in cartilage organ cultures. Static compression has been found to decrease proteoglycan and protein synthesis (Gray et al., 1988; Sah et al., 1989; Schneiderman et al., 1986), while dynamic compression at certain frequencies and amplitudes stimulated synthesis of these matrix constituents (Korver et al., 1992; Parkkinen et al., 1992; Sah et al., 1989). These data imply that the presence of physiologic mechanical loading forces may be necessary for the proper assembly and maintenance of a matrix that can function in the joint.

Chondrocytes cultured in an agarose gel maintain the expression of aggrecan (cartilage-specific large aggregating PG) and collagen types characteristic of articular cartilage (predominantly collagen II as well as types IX and XI) (Aydelotte et al., 1988; Benya and Shaffer, 1982; Sun et al., 1986). The maintenance of chondrocyte phenotype during long-term culture in agarose gels allowed the development of a mechanically functional cartilage-like matrix (Buschmann et al., 1992). The equilibrium modulus, dynamic stiffness, and oscillatory streaming potential rose to many times (>5×) their initial values at the start of the culture; the hydraulic permeability decreased to a fraction (~1/10) that of the cell-laden porous agarose at the beginning of the culture. In the present study we addressed the question of whether mechanical loading of chondrocyte/agarose cultures could affect the rate of synthesis of matrix macromolecules. We report that chondrocytes in agarose gel respond biosynthetically to static and dynamic mechanical loads in a manner similar to that of intact organ culture. However, the response to compression was more pronounced at later times in culture after the level of matrix development was more advanced. Application of mechanical loads in a culture environment may therefore significantly alter the long-term development of this tissue, and may shed light on the physiological events and cellular mechanisms by which chondrocytes respond to mechanical signals in vivo.

MATERIALS AND METHODS

Isolation of chondrocytes and agarose gel culture

Saddle sections (~8 kg) from 1-2 week old calves were obtained from a local abattoir (A. Arena, Hopkinton, MA) within 3-4 hours after slaughter. The intact femoropatellar groove was isolated as described previously (Sah et al., 1989). The region between the lateral and medial ridges of the groove was removed as one piece from the underlying bone. After being cleaned of any bone and fibrous material, the tissue (19-26 g) was diced into approximately 1 mm^3 pieces and cultured in feed medium (DMEM, high glucose, supplemented with 0.1 mM nonessential amino acids, 0.4 mM proline, 2 mM glutamine, 100 U/ml penicillin G, 100 μg/ml streptomycin, 10 μg/ml ascorbate (Gibco), and 10% FBS (Hyclone, Logan, UT)) at 37°C in 5%CO_2:95% air. Medium (8 ml/g tissue) was changed daily and 4-6 days later cells were extracted by sequential pronase/collagenase digestion (Kuettner et al., 1982). Cartilage pieces were immersed in DMEM with 1% (w/v) pronase (Sigma P5147) and shaken gently for 1 hour at 37°C. They were then washed in PBS (with 0.9 mM $CaCl_2$ and 0.5 mM $MgCl_2$) and shaken gently in DMEM with 5% serum and 0.4% (w/v) bacterial collagenase (Worthington, type 2) for 4 hours at 37°C. Cells were isolated from the digest by centrifugation for 10 minutes at 100 ***g***, resuspended, and passed through a 100 μm nylon filter (Spectrum, Los Angeles). The cells were centrifuged and resuspended again, and passed through a 20 μm filter. Cells were centrifuged again and resuspended in feed medium (but with no ascorbate) in a 300 ml non-vented T-flask so that no air was present in the flask. The flask was stored overnight at 4°C.

Total cell number was determined using a Coulter counter, and cell viability was determined with Trypan Blue exclusion on a hemocytometer. Chondrocytes were then centrifuged, resuspended in DMEM and mixed with an equal volume of PBS containing low melting temperature agarose (SeaPlaque agarose, FMC Bioproducts, Rockland, ME) (Aydelotte et al., 1986; Sun et al., 1986) at 37°C to yield ~2×10^7 cells/ml in 2% or 3% (w/v) agarose and cast between slab gel electrophoresis plates separated by 1 mm thick Teflon spacers (Buschmann et al., 1992). After gelling at 0°C for 5 minutes followed by 4°C for 2-6 hours, approximately 100 disks, 16 mm in diameter by 1 mm thick, were cored from the slab gels using a stainless steel punch. The chondrocyte/agarose disks were subsequently cultured on top of 1 mm pore size nylon mesh (Spectrum, Los Angeles) to promote nutrient diffusion from below and above. Each disk was fed 2 ml per day of medium (as above but with 50 μg/ml ascorbate) up to day 16, then 2.5 ml per day up to day 22, 3 ml up to day 32, and then 4 ml up to day 47. Agarose disks without chondrocytes were prepared and maintained in a similar manner. The data presented below represent a compilation of three cultures, of length 47 days, 35 days, and 28 days. Chondrocytes were cast in 2% and 3% agarose for the 47 and 35 day cultures while only 3% gels were made for the 28 day culture. The cell population for each culture was obtained from the two femoropatellar grooves of one animal.

Chambers for compression-radiolabel experiments

The chambers for static and dynamic compression, shown schematically in Fig. 1, have been described previously (Sah et al., 1989). The compressed thickness of the chondrocyte/agarose (CA) disks in the static chamber was set by placing teflon spacers between the chamber lid and base and applying a weight to the chamber lid, forcing the lid, spacer, and base together. These chambers could accommodate 12 specimens compressed to the desired thickness. A range of compression levels was achieved by using multiple chambers with spacers of different thicknesses. The static chambers were used in a tissue culture incubator and had small lateral channels in their bases allowing incubator gas to equilibrate with the medium. The total time to assemble and load each chamber was ~5-10 minutes.

For the dynamic chamber, compression was applied with a mechanical spectrometer (Dynastat, IMASS, Hingham, MA). A sterile tissue culture environment was maintained inside the chamber by recirculating the medium through a controlled heat exchanger (37°C) and by passing a humidified mixture of 5% CO_2:95% air through a 0.22 μm filter into the chamber above the fluid level. The dynamic chamber accommodated 24 specimens, 12 of which were statically compressed to 0.73 mm thickness (from 1.00 mm) using a set of pins fixed to the chamber lid. The other 12 specimens were compressed using the mechanical spectrometer via sliding rods in the chamber lid. They were initially compressed to the 0.73 mm static offset over which a sinusoidal displacement of 30 μm amplitude was superimposed. The dynamic chamber was slightly modified for experiments with chondrocyte/agarose disks: (1) the dynamic compression rods were hollowed out to ensure that the weight of the rods alone would not significantly compress the specimens; and (2) the medium was stirred inside the chamber using a motor-driven stir bar. The stirring helped

to eliminate temperature and pH gradients within the chamber and stagnant layers at the perimeter of the CA disks.

The mechanical Spectrometer was interfaced to a computer and a frequency synthesizer (Model 5100, Rockland Systems, West Nyack, NY) to control the applied compressive displacement (accuracy <1 μm). During culture experiments, the displacement and resulting load were recorded on a chart recorder and/or digitized and stored on a computer. Fourier decomposition of the load signal into fundamental and higher harmonic components enabled quantitative assessment of non-linearities. The total time to load CA disks into the dynamic chamber under sterile conditions, seal the chamber, mount it in the spectrometer, and begin compression was ~30 minutes.

Compression and radiolabeling protocols

Twelve 3 mm diameter CA disks were cored out of each 16 mm disk used in compression-radiolabel experiments with a stainless steel dermal punch (Miltex Instruments, Lake Success, NY). These 3 mm disks were then placed in culture dishes with prelabel medium (DMEM, low glucose, 10% FBS, 10 mM HEPES, 0.1 mM nonessential amino acids, 0.4 mM proline, 100 U/ml penicillin G, 100 μg/ml streptomycin, and 20 μg/ml ascorbate). The dishes were placed in a standard incubator for 16-30 hours prior to compression.

Static mechanical compression

Forty-eight 3 mm disks cored from four larger 16 mm disks were removed from the prelabel dishes and loaded into 4 different static compression chambers with medium as above (0.78 ml per well; 1 disk per well) but containing 10 μCi/ml [^{35}S]sulfate and 20 μCi/ml [5-^{3}H]proline to assess the rates of GAG synthesis and amino acid uptake and protein synthesis, respectively. The static chambers were assembled with spacers to achieve final compressed thicknesses between 0.4 mm and 1.0 mm. After culturing the disks for 16 hours under compression, the specimens were removed from the chambers and analyzed for rates of radiolabel incorporation, GAG content and DNA content (see below). Free-swelling disks (1.00-1.09 mm thickness depending on the day of culture) were also incubated in 48-well dishes, 1 disk per well, alongside the compressed specimens.

Dynamic mechanical compression

Twenty-four 3 mm disks cored from two 16 mm disks were removed from the prelabel dishes and loaded into the dynamic chamber containing labeled medium (as above but with 20 ml in the single well containing all 24 3 mm disks) to provide 12 experimental dynamically compressed specimens and 12 controls. Experimental disks were subjected to oscillatory compression of 30 μm amplitude (60 μm peak-peak) superimposed on a static offset compression of 0.73 mm at one of the following frequencies: 0.001 Hz, 0.01 Hz, 0.1 Hz, 1.0 Hz. Control disks were held statically at 0.73 mm. Dynamic compression in the presence of radiolabel continued for 10 hours at which time the disks were removed from the chamber and analyzed for rates of incorporation, GAG content and DNA content (see below). Zero-displacement control experiments were also performed in which no sinusoidal displacement was applied to the dynamic compression rods.

Biochemical analysis of rates of incorporation, GAG content, DNA content

After each compression experiment in the presence of radiolabel, the disks were washed 6 times over 2 hours in cold PBS (with ~1 mM unlabeled sulfate and proline but without $CaCl_2$ or $MgCl_2$). In one set of experiments designed to quantify the spatial variation in radiolabel incorporation, 2 mm diameter centers were cored after washing the 3 mm CA disks and analyzed separately from the 3 mm rings. Disks were then lyophilized and digested in 1 ml/disk papain (Sigma P3125, 125 μg/ml in 0.1 M sodium phosphate, 5 mM Na_2-EDTA, and 5 mM cysteine-HCl, pH 6.5) for 16 hours at 60°C. The agarose was melted at 70°C for 10 minutes, immediately followed by vortexing. Portions (100 μl) of the digest were analyzed for radioactivity by mixing with 100 μl of 10% SDS and 2 ml Scinti-Verse Bio-HP (Fisher) and measuring [^{3}H]cpm and [^{35}S]cpm in a liquid scintillation counter (Rack-Beta 1211, LKB, Turku, Finland), with corrections for spillover and dilution quenching. For some of the disks, the macromolecular fraction of incorporated sulfate was determined by applying 0.5 ml of the digest to a PD10 column of Sephadex G-25 (M_r cutoff of 1,000-5,000; Pharmacia, Piscataway, NJ) and eluting with 2 M guanidine-HCl. Fractions (0.5 ml) were collected and counted, or alternatively, the macromolecular (V_0) and low molecular mass component peaks were pooled and counted. The content of sulfated GAG remaining in the disks was assessed by reaction of 20 μl portions with 200 μl Dimethylmethylene Blue dye (DMB) solution (Farndale et al., 1986) in 96-well microplates (Nunc) and spectrophotometry (model Vmax plate reader, Molecular Devices, Menlo Park, CA); chondroitin sulfate (0-2 μg of shark cartilage, Sigma) was used as a standard. The DNA content within the disks was measured by reaction of 100 μl portions of the digest with 2 ml Hoechst 33258 dye solution in an acrylic cuvet and fluorometry, using calf thymus DNA as a standard (Kim et al., 1988). GAG lost to the medium during culture was assessed by reacting 20 μl portions of feed medium (every second day up to day 37) in 200 μl DMB solution as above; no interference from serum or medium was observed. Aliquots of the labeled medium from static compression experiments were also separated on PD10 columns to obtain macromolecular counts in the medium which diffused out during the 16 hour labeling period.

Histological analysis

Whole 16 mm disks were removed from culture and fixed in 2% (v/v) glutaraldehyde solution buffered with 0.05 M sodium cacodylate, and containing 0.7% (w/v) of ruthenium hexaammine trichloride (RHT) (Hunziker et al., 1982). Fixation was effected initially at ambient temperature (6 hours) and subsequently at 4°C (12 hours). Disks were then washed in 0.065 M NaCl and 0.1 M sodium cacodylate (pH 7.4) and stored in 70% ethanol at 4°C. Following dehydration in a graded series of increasing ethanol concentrations, specimens were embedded in Epon 812 which was polymerized at +60°C. Semi-thin (1 μm) sections, prepared for analysis in the light microscope, were stained with Toluidine Blue 0. Thin sections stained with uranyl acetate and lead citrate were utilized for electron microscopic analysis in a Hitachi H7100-B electron microscope.

Physical characterization

The mechanical and electromechanical properties of 13 mm chondrocyte/agarose disks and control disks with no cells were measured as described in (Buschmann et al., 1992). Briefly, 13 mm diameter disks were tested in confined compression geometry using the mechanical spectrometer. The disk was placed in a tight-fitting confining cylindrical well inside a nonconducting chamber filled with PBS and equipped with silver/silver-chloride disk electrodes to measure the compression-induced uniaxial streaming potential. A porous compressing platen was placed on top of the specimen and brought into contact with the upper post of the spectrometer. Both equilibrium and dynamic mechanical tests were performed. A sequence of step compressions (0.5%) was applied from 0-20% compression. Stress-relaxation between steps was allowed to equilibrate before collecting the equilibrium load and proceeding to the next step. Once a 20% static offset was obtained, a small amplitude (5-7 μm) sinusoidal displacement was applied at frequencies between 0.01 and 1.0 Hz. The amplitude and phase of the displacement, load, and streaming potential were determined from the digitized data.

RESULTS

Time evolution of GAG and DNA content and biosynthetic rates

The rates of GAG and DNA accumulation within the disks

during the 3% agarose 47 day culture are shown in Fig. 2. These data are from one of the three culture experiments described here, but are representative of the 3% agarose specimens from all three cultures. GAG concentration (mg/ml-disk-volume) increased many-fold and DNA concentration increased by ~35% over the 47 day culture period. By 30-45 days in culture, both GAG and DNA concentration had reached ~1/4 that of the 'parent' calf cartilage tissue.

The measured [^{35}S]sulfate and [^{3}H]proline incorporation during 16-hour radiolabeling of these same free-swelling disks are shown versus time in culture in Fig. 2. The corresponding rates of sulfate and proline incorporation are also shown (nmol/10^6 cells per day), calculated assuming identical intracellular and extracellular specific activities and normalized to cell number using 7.7 pg DNA/cell (Kim et al., 1988). In general, the sulfate and proline incorporation levels in chondrocyte/agarose culture were initially higher (before day 30) and subsequently similar to that in the intact articular cartilage (Fig. 2). For the 47 day culture where both 2% and 3% agarose specimens were prepared, the incorporation rates in 2% agarose (not shown) were higher (~50%) than those in 3% agarose (Fig. 2) on day 3 but by day 12 the rates were not significantly different in cultures from the same animal. The rate of release of GAG to the medium (not shown) from the large 16 mm disks increased approximately linearly from day 0 to day 10, after which time the rate remained constant at (36.2±4.9) μg/disk per day for 2% agarose and (31.3±4.3) μg/disk/day for 3% agarose (mean ± s.d.; n=12 for each). The reduced rate of release in 3% agarose compared to 2% agarose seemed to compensate for the lower initial synthetic rate, and later in culture (day 20-47) was consistent with a slightly higher GAG concentration in the 3% agarose disks (Fig. 2) by 14±5% compared to 2% agarose specimens (not shown). The disks swelled in the axial direction by 5-10% over 47 days with no apparent difference between 2% and 3% agarose specimens (not shown). This swelling is most likely the result of the deposition of proteoglycan and its associated electrostatic swelling forces (Buschmann and Grodzinsky, 1995).

Morphological development

Chondrocytes fixed within a few hours after seeding (day 0) in agarose were homogeneously dispersed, essentially denuded of matrix, and structurally disorganized (Fig. 3A and B, and Fig. 4A and B). After 1 day of culture, the cells regained a normal morphological appearance, had synthesized a thin halo of pericellular matrix, and had expanded in volume (Fig. 3C and D, and Fig. 4C and D). By 6 days of culture, the cell-associated matrix had grown substantially and continued to expand thereafter (Fig. 5). Even though Toluidine Blue stained light microscopic sections suggested an apparent absence of matrix in the lightly stained interterritorial areas at later times (e.g. Fig. 5), preliminary electron microscopic evaluation (not shown) revealed the presence of matrix granules in this region. In addition the agarose seemed to be excluded from the darkly stained pericellular region and pushed away from the expanding matrix coat into a compact form immediately outside the pericellular coat. The lightly stained matrix outside this region appeared to be integrated with the agarose.

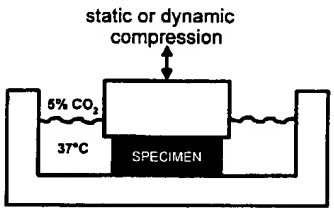

Fig. 1. Schematic of chambers used in the compression-radiolabel experiments.

Physical properties

The confined compression equilibrium modulus, H_A (a measure of the static equilibrium stiffness of the tissue) and the hydraulic permeability k (a measure of the ease of fluid flow through the material) were obtained from measurements of the dynamic stiffness of 13 mm diameter disks in the frequency range 0.01-1.0 Hz, as described by Buschmann et al. (1992). Fig. 6 shows that the modulus increased and the permeability decreased as the culture progressed and matrix was deposited in 3% agarose specimens. The streaming potential is a measure of the intratissue electric field produced by compression-induced fluid flow convecting counterions past fixed charge groups on the proteoglycans. The magnitude of these electric fields increased several fold during the 47 day culture (Fig. 6). The time evolution of these physical properties is qualitatively similar to that seen in (Buschmann et al., 1992) for 2% agarose. By day 28, the modulus and streaming potential were ~1/5 those of the 'parent' cartilage and the permeability was about twice that of the 'parent' tissue. The average modulus of the 3% control gel disks with no cells was 17.7±2.7 kPa (Fig. 6)

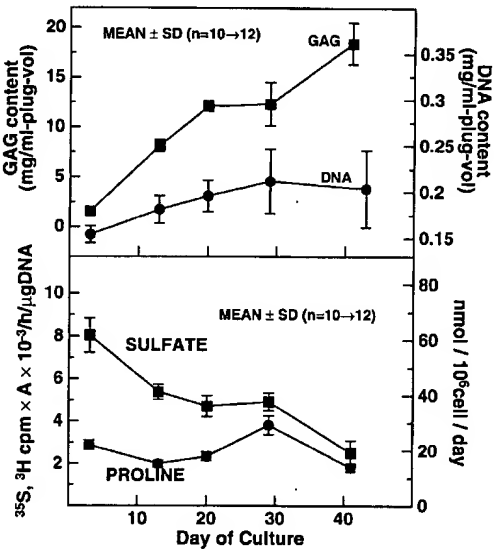

Fig. 2. Top: GAG and DNA concentration in 3 mm diameter chondrocyte/agarose disks versus time during a 47 day culture, in mg per ml of disk volume using 3% agarose. Disk volume increased by 5% to 10% during culture. Bottom: Sulfate and proline incorporation versus time in culture using 3% agarose. A = 1.36±0.04 for sulfate, 0.285± 0.008 for proline.

compared to 13.1±2.8 kPa for the 2% controls shown by Buschmann (1992) (mean ± s.d.; n=4,5). The hydraulic permeability of the 3% agarose control gels was $36.9\pm4.6\times10^{-15}$ $m^4/(N.s)$ compared to $51.4\pm8.5\times10^{-15}$ $m^4/(N.s)$ for 2% agarose control gels.

Biosynthetic response to static and dynamic compression in whole 3 mm diameter disks

The following results pertain to chondrocytes in 3% agarose unless otherwise indicated. At early times in culture (day 2) when little matrix has yet accumulated (Fig. 2), static compression of CA disks from a free swelling thickness of 1.00 mm down to 0.52 mm did not significantly alter the rate of [^{35}S]sulfate incorporation (Fig. 7). After 41 days of culture and the accumulation of ~1/4 the matrix content of 'parent' disks, there was a dose-dependent decrease in [^{35}S]sulfate incorporation rate with increasing compression (Fig. 7). The incorporation rate at 0.52 mm disk thickness was 22±13% lower than disks held at 0.95 mm and significantly lower than that of disks taken from day 2 of culture and compressed to the same 0.52 mm thickness. [^{3}H]proline incorporation followed similar trends. At later times, the accumulation of matrix in CA disks

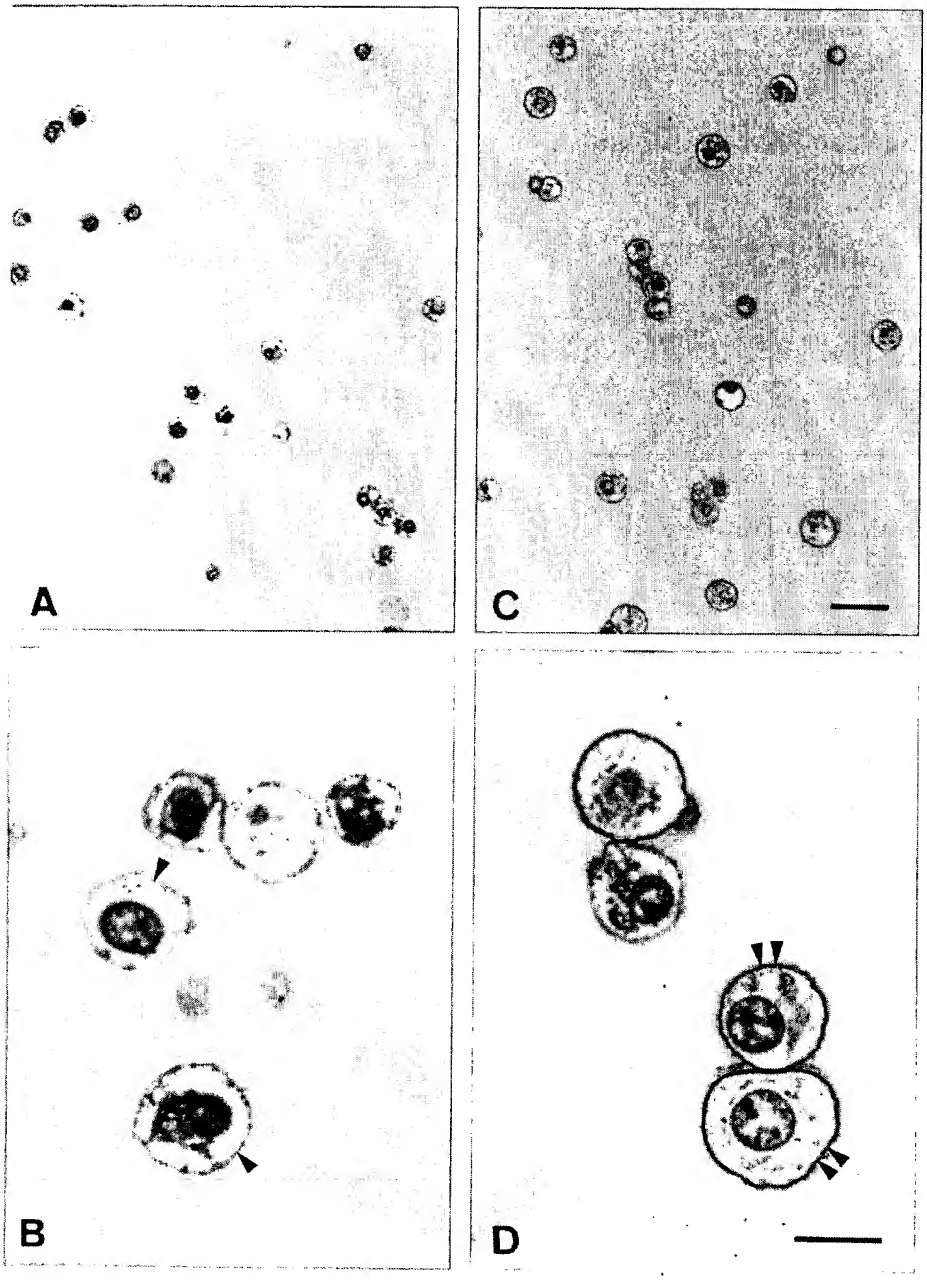

Fig. 3. (A and B) Agarose gels containing freshly seeded chondrocytes were fixed within 4 hours after gels were cast (day 0). (C and D) Agarose gels containing chondrocytes which were fixed on day 1 of culture, approximately 24 hours after seeding. Cells are homogeneously dispersed as individual cells or in groups of 2 or 3 cells after gel casting ($\simeq15\times10^6$ cells/ml). Immediately after casting chondrocytes appear shrunken and contain a disorganized cytoplasm (A and B). After 1 day of culture (C and D) a thin matrix coat has been generated and the cells are expanded with a more structured cytoplasm. Single arrowheads - cell membrane with no identifiable matrix coat. Double arrowheads - cell membrane with associated matrix coat. Thick sections (1 μm) stained with Toluidine Blue-O. (A and C) Same magnification: bar, 25 μm. (B and D) Same magnification: bar, 10 μm.

allowed for greater compression since the presence of matrix helped to retain disk integrity. At early times, compression further than 0.5 mm resulted in cracking of the agarose. Static compression of chondrocytes in 2% agarose showed very similar results (not shown).

PD10 analysis of papain digested 3 mm diameter disks

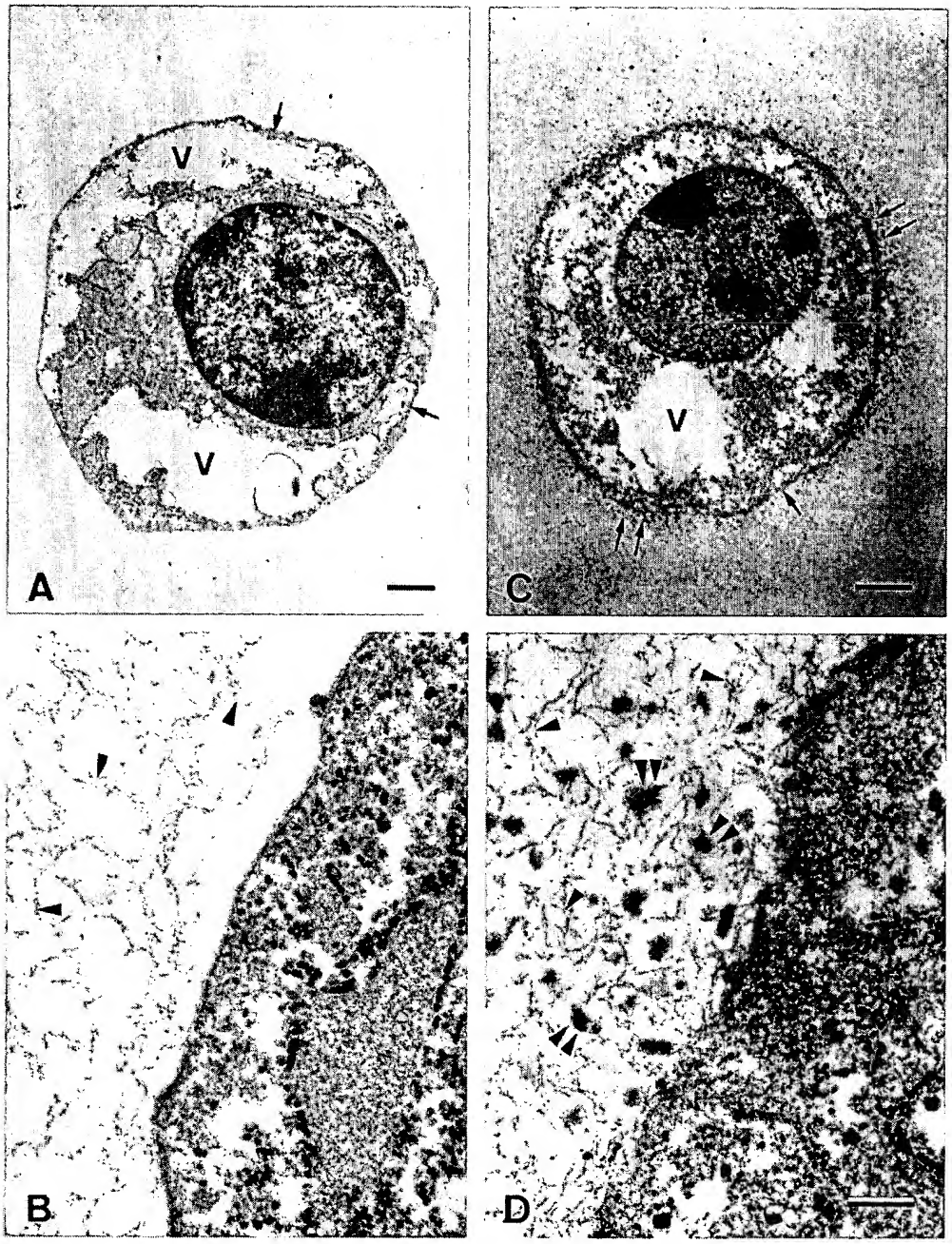

Fig. 4. Electron micrographs of individual cells on day 0 (A) and day 1 (C) of culture and the cell/matrix interface on day 0 (B) and day 1 (D) of culture. The cell fixed immediately after seeding (A) contains more prominent vacuolar space (V) than after 1 day of culture (C). The enzymatic digestion to isolate chondrocytes from cartilage has entirely removed any cell-associated matrix (B). Granules of newly synthesized matrix (paired arrowheads) have been incorporated into the agarose gel (single arrowheads) surrounding the chondrocytes after 1 day of culture (D). Single arrow - plasmalemma. Double arrows - pericellular matrix. Glutaraldehyde fixation in the presence of RHT. Section staining with uranyl acetate and lead citrate. (A) Bar, 1 μm. (C) Bar, 2 μm. (B and D) same magnification: bar, 0.2 μm.

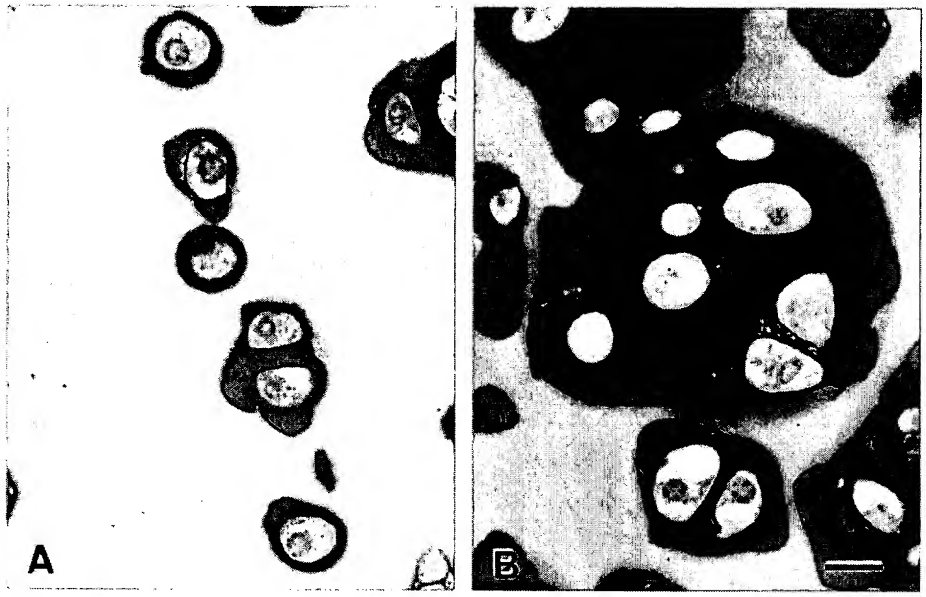

Fig. 5. Chondrocyte/agarose cultures after 6 (A) and 27 (B) days of culture. Representative light micrographs of Toluidine Blue stained 1 μm sections from early and late times in culture when mechanical compression experiments were performed. The more highly developed matrix on day 27 is required for the transduction of mechanical compression of these gels to a cellular biosynthetic response. (A and B) Same magnification: bar, 15 μm.

indicated that 99.2±0.5% of the total [^{35}S]sulfate in the disks was macromolecular (n=4). PD10 analysis of the media from disks that were statically held at 1.00 mm indicated that 1.4±0.6% of the total incorporated macromolecular [^{35}S]sulfate had diffused out into the medium during the 16 hour label.

At early times in culture (days 2-5) there was a small increase (6-13%) in the rate of [^{35}S]sulfate incorporation in the dynamically compressed CA disks when compared to controls held at the same static offset thickness (Fig. 8). At later times the rate of [^{35}S]sulfate incorporation in the dynamically compressed CA disks was 15%-25% greater than that of the static controls. Proline incorporation followed similar trends with levels of stimulation being somewhat higher than sulfate, 10-20% at early times and 10-35% at late times. The apparent increase in stimulation with frequency seen in Fig. 8 could be partially due to the 1.0 Hz experiment being done at 41 days (in the 47 day culture) compared to 23 days for the 0.1 Hz and 0.01 Hz experiments (in the 35 day culture). Only two experiments were performed at 0.001 Hz. A day 13 experiment resulted in a stimulation of sulfate incorporation of 1.128±0.118 (P<0.05) in dynamically compressed specimens relative to static controls, while a day 24 experiment revealed an inhibition of 0.937±0.70 (P>0.05). During the 10 hour compression-labeling period, ~36,000 cycles were completed at 1 Hz, ~3,600 at 0.1 Hz, ~360 at 0.01 Hz, and ~36 at 0.001 Hz. For 3% agarose specimens, the amplitude of the measured sinusoidal load decreased during the 10 hour constant compression-radiolabel experiments due to fatigue of the specimens. At early days of culture the load amplitude decreased by 15-50% during the 10 hours of applied compression, and at later times it decreased by 10-30%. The nonlinearity in the measured load increased from ~5% THD (total harmonic distortion) at the beginning of compression to ~50% THD after 10 hours at early times in culture. At later times in cultures, the final value of the THD was ~30%. The response of chondrocytes in 2% agarose to dynamic compression was variable, perhaps due to its lower stiffness and greater fatigue during repeated compression. Analysis of GAG and DNA

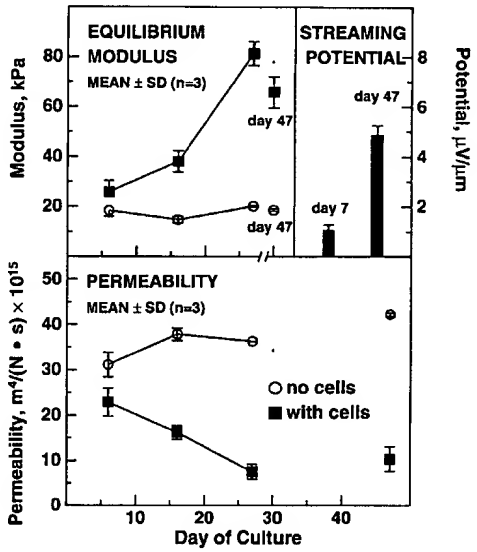

Fig. 6. Equilibrium confined compression modulus, H_A, and hydraulic permeability, k, of chondrocytes in 3% agarose disks versus time in culture, compared to control 3% agarose disks with no cells. The points connected by lines are from a 28 day culture while the day 47 points are from a different 47 day culture. These were calculated from the dynamic stiffness measured in the frequency range (0.01 Hz-1.0 Hz) using a model (Frank and Grodzinsky, 1987) based on the linear KLM biphasic theory (Mow et al., 1980). The streaming potential of chondrocyte/agarose disks at two different days from the 47 day culture are also shown.

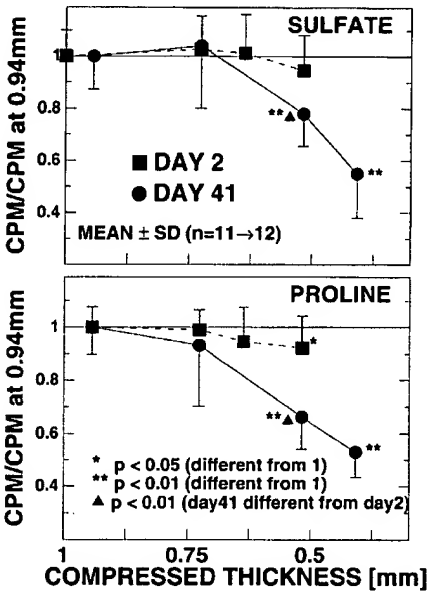

Fig. 7. Rate of incorporation of [^{35}S]sulfate and [^{3}H]proline in 3 mm diameter chondrocyte/3% agarose disks subjected to increasing levels of static compression. Chondrocyte/agarose disks were from day 2, before the accumulation of matrix, and day 41 after the accumulation of matrix (Fig. 2). The compression was applied using the chamber in Fig. 1, in unconfined geometry with impermeable platens.

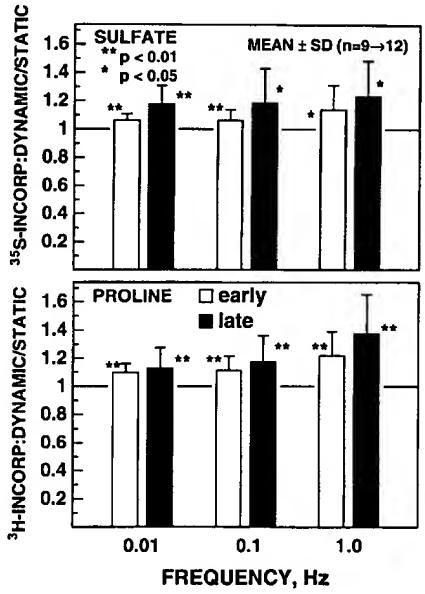

Fig. 8. Rate of [^{35}S]sulfate and [^{3}H]proline incorporation in 3 mm chondrocyte/3% agarose disks subjected to a 30 μm dynamic oscillatory displacement, normalized to disks held statically at the offset thickness of 0.73 mm. Disks were from early time (day 5 for 0.01 Hz and 0.1 Hz, day 2 for 1.0 Hz) in culture - open bars - and late time (day 23 for 0.01 Hz and 0.1 Hz, day 42 for 1.0 Hz) - solid bars. p values were computed using the two tailed t-test for dynamically compressed specimens compared to controls (static). The stimulation in [^{35}S]sulfate incorporation at later times of culture for dynamically compressed disks at 0.01 Hz is significantly higher than the stimulation at early time (p<0.05).

content showed no significant differences between the dynamically compressed disks and control disks, for all experiments, with 2% and 3% agarose.

Zero-displacement controls using the dynamic chamber were performed with the dynamic chamber in an identical fashion, but with no applied displacement. In two such experiments, the relative rates of [^{35}S]sulfate incorporation in the disks under the dynamic pins and those under the static pins were 1.006±0.112 and 1.048±0.047. For [^{3}H]proline the relative rates were 1.066±0.042 and 1.057±0.069 (mean ± s.d.; n=10-12).

Spatial variation of biosynthetic response to static and dynamic compression: 2 mm center vs 3 mm ring

In order to elucidate possible mechanisms involved in the inhibition of biosynthesis under static compression and the stimulation of biosynthesis with dynamic compression, experiments were done in which the 2 mm center and 3 mm outer ring of each 3 mm diameter disk were analyzed separately for incorporation rates, DNA content and GAG content. Fig. 9 shows that the inhibition in [^{35}S]sulfate incorporation rate produced by static compression was greater in the center of each disk than in the outer ring. The incorporation rates plotted in Fig. 9 are those of the center of each disk relative to the center held at 0.95 mm and those of the rings of each disk relative to the ring held at 0.95 mm. The total incorporation rates for the whole 3 mm disk were calculated from the center and ring of each disk. The inhibition in the center and the difference between the center and the ring increased with time in culture for experiments done on day 3, day 13, and day 24, in a dose dependent manner. At the levels of compression shown in Fig. 9 the incorporation rates in the ring were not affected while on day 24 the center was depressed by 20±18% when compressed to 0.637 mm. Incorporation rates in free-swelling specimens were not different from those held between impermeable platens at 0.95 mm thickness, near the free-swelling thickness of 1.00-1.09 mm. [^{3}H]proline incorporation followed very similar trends (data not shown). 2 mm centers were not cored on day 3 from disks compressed to 0.64 mm since small cracks in the disks prevented accurate coring. At later times disk integrity was maintained due to the accumulation of matrix.

The magnitude of stimulation of synthesis in dynamically compressed specimens was greater at later times than earlier times as seen in Fig. 8 and it was also greater in the outer ring than in the center. The difference between the ring and center increased with culture time and deposition of matrix. In Fig. 10 the rate of incorporation of the ring relative to the center of each disk is plotted for dynamically compressed specimens and static controls on day 4, 14, and 25. At early times (day 4) there is no difference in sulfate incorporation rate between the ring and the center in either the experimental or control disks. On day 25 the incorporation rate is higher in the ring for both the experimentals and controls. The 9% increase in the ring relative to the center on day 25 for the control held at a static

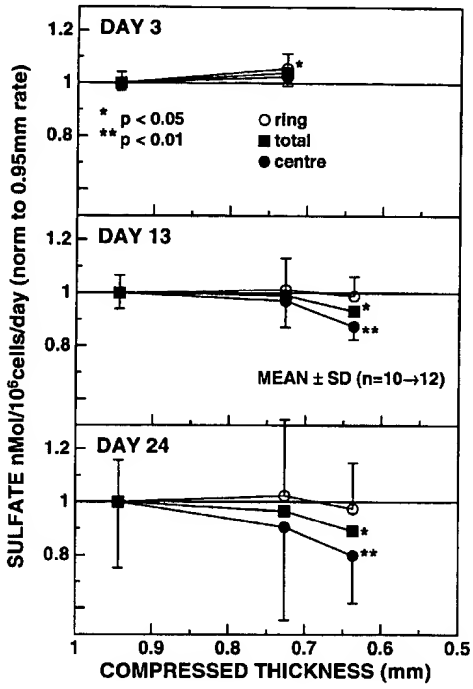

Fig. 9. Rate of incorporation of [^{35}S]sulfate in the 2 mm diameter centers and 3 mm diameter rings of chondrocyte/3%agarose disks subjected to increasing levels of static compression. Chondrocyte/agarose disks were from day 3, day 13, and day 24 of culture. The incorporation rates of the centers on each day are normalized to that of the center from the disk compressed to 0.95 mm on that day. The rings on each day are normalized to the incorporation rate of the ring from the disk compressed to 0.95 mm on that day. Proline incorporation rates showed similar trends.

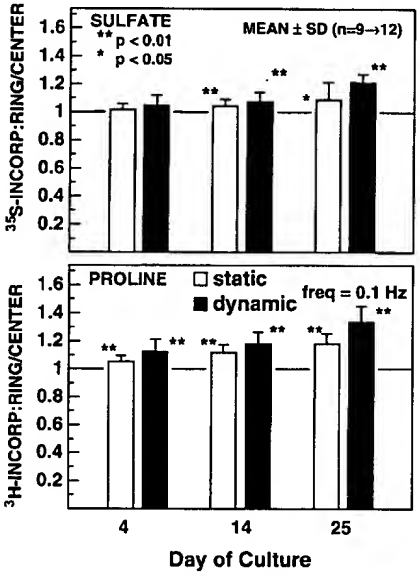

Fig. 10. Rate of incorporation of [^{35}S]sulfate and [^{3}H]proline in the 3 mm-diameter ring normalized to the 2 mm diameter center of chondrocyte/3%agarose disks subjected to a 30 μm dynamic oscillatory displacement at 0.1 Hz and disks held statically at the offset compression of 0.73 mm. Chondrocyte/agarose disks were from day 3, day 13, and day 24 of culture.

offset thickness of 0.73 mm is consistent with static compression experiments shown in Fig. 9. For the experimental disks the incorporation rate in the ring was 21% higher than the center, a difference which was only partially (~1/2) accounted for by the greater inhibition in the center with a static compression of 0.73 mm. The rings were then preferentially stimulated by dynamic compression compared to centers.

DISCUSSION

Articular chondrocytes grown in three-dimensional agarose gel cultures exhibit a biosynthetic response to deformation of the gel-cell-matrix system. The intensity of the response increases with increasing time of culture and therefore with the degree of matrix development, suggesting a fundamental role of the ECM in signal transduction. Static (equilibrium) compression results in a depression in synthesis of proteoglycans and proteins while small amplitude oscillatory dynamic compression stimulates synthetic rates. Intact cartilage explants respond to these loading regimes in a qualitatively similar manner (Sah et al., 1989). Chondrocytes cultured in agarose gel therefore not only express molecular and morphological characteristics of the chondrocyte phenotype but also respond to mechanical loading in a way similar to that of chondrocytes in organ culture and in vivo. In view of the fact that matrix development tends to be localized to within a few cell diameters around cells or cell-groups in agarose, it is suggested that the minimal system exhibiting typical responses to mechanical loading for chondrocytes includes the cell and its immediate pericellular matrix. The flexibility of the agarose system is particularly suited to the localization of transduction events within this tissue region.

Biosynthetic response to static compression

The inhibition of sulfate and proline incorporation rates caused by static compression was dependent on the day of culture and, therefore, the presence of matrix in chondrocyte/agarose disks. Without matrix, at early times in culture, little or no change in response to compression was observed (Figs 7 and 9). As matrix developed, the inhibition in biosynthesis was enhanced (Figs 7 and 9). Comparison with a previous study (Sah et al., 1989) using the calf 'parent' cartilage explants shows that by 41 days in culture when the GAG concentration in chondrocyte/agarose disks was ~1/4 that of the 'parent' cartilage disks, the relative depression in biosynthesis with compression was also ~1/4 of that seen in the calf cartilage disks. However, the slopes of the two curves of synthetic rate vs compressed thickness are similar in the regions where inhibition of synthesis is occurring. The chondrocyte/agarose system may require some initial compression to attain a 'physiological static offset' after which the response is more quantitatively similar to intact cartilage. The spatial variation in biosynthetic

response also exhibited a dependence on the level of matrix present in the disks. The 2 mm diameter central region of 3 mm disks was more strongly affected than the 3 mm diameter ring, and this difference became accentuated as the culture progressed and more matrix was deposited (Fig. 9). This spatial variation has also been observed with cartilage (Kim et al., 1994b).

Possible mechanisms involved in the transduction of static compression to a signal sensed by chondrocytes may be categorized as: (1) cell deformation, (2) transport-related, (3) physicochemical, and (4) cell-matrix interactions. Previous studies (Freeman et al., 1994; Lee and Bader, 1994) and ongoing work by us indicates that deformation of the agarose gel does result in cell-deformation. However, changes in cell shape and volume tend to be larger when less matrix is present (i.e. at early times in culture), opposite to the change in magnitude of the biosynthetic response with time in culture observed here. Numerous previous studies have also examined the possible role of transport limitations resulting from a reduction in the average pore size of the matrix under compression (Kim et al., 1994; Schneiderman et al., 1986; Tomlinson and Maroudas, 1980). The majority of these results to date have suggested that limitations in the availability of nutrients (e.g. oxygen, sulfate, growth factors etc.) is not solely responsible for the observed inhibition of biosynthesis in compressed cartilage. Transport related mechanisms may also appear less likely in light of Fig. 9. There were no center/ring differences in disks held at 0.95 mm thickness at any time in culture, early or late. Furthermore, there was no difference in biosynthetic rates between free-swelling disks and those with the top and bottom surfaces covered at 0.95 mm thickness (data not shown). If transport limitations were significant, some center/ring differences could be expected to appear in the specimens held at 0.95 mm as the culture progressed. Physicochemical mechanisms are related to the decrease in hydration with compression and the resulting increase in fixed charge density (FCD) associated with the presence of ionized charge groups on the proteoglycans. This increase in negative FCD increases intra-disk concentrations of cations such as Na^+ and H^+, thereby increasing the osmotic pressure and reducing the pH. Reduced extracellular pH has been seen to reduce cellular biosynthetic rates (Gray et al., 1988); however, longer term effects of pH changes and tissue compression were seen to be different (Boustany et al., 1994). The importance of physicochemical events in the chondrocyte/agarose system cannot be definitively ascertained on the basis of these studies and our present work.

Fig. 4 shows the beginnings of a substantial development in pericellular matrix. The granules in these electron micrographs are most likely condensed proteoglycans precipitated by the actions of the cationic dye ruthenium hexaammine trichloride and the chemical fixative. Proof of a collagen fibrillar network is difficult to find at the EM level in these micrographs due to the disruptive effects of the fixative. However, previous biochemical characterization of similar cultures has indicated that collagen, predominantly type II, is synthesized and deposited in the gel (Buschmann et al., unpublished results). We also have preliminary evidence using high-pressure freezing fixation that a fine fibrillar network is present. It is possible that specific connections between the chondrocyte and this pericellular matrix are required for the cellular response to mechanical stimuli. The increased responsiveness of the chondrocyte/agarose cultures with increasing time in culture could be partially a result of the development of the necessary transduction machinery at the cell-matrix interface, and potentially throughout the matrix (Fig. 5). It may be reasonable to assume that the chondrocyte itself is in a state of mechanical 'readiness' after day 1 given its apparently normal morphology after this time (Fig. 3). Although the molecular constituents of the chondrocyte-matrix interface are only beginning to be characterized, some components have been identified: β_1 integrins including α_2, α_3, α_5, α_6 and α_v (Durr et al., 1993; Enomoto et al., 1993) and the hyaluronan receptors, CD44, RHAMM, and TSG-6 (Flannery and Sandy, 1994; Hardingham and Fosang, 1992; Knudson and Knudson, 1993). Cell-matrix interactions could have important roles in the transduction of mechanical signals, analogous to those seen in development and differentiation (Adams and Watt, 1993). The role of integrins in mechanotransduction of other cell types is well-established (Ingber, 1991). It remains to be elucidated which if any of these receptors or intracellular structural alterations are important in the mechanical feedback system operant in cartilage.

Biosynthetic response to dynamic compression

A small stimulation in biosynthesis (6-13%) was observed in CA disks at early times in culture. At later times in culture, the level of stimulation in sulfate incorporation increased to 15-25%. The level of stimulation seen in calf cartilage disks under similar conditions was 20-40% (Sah et al., 1989). Therefore the stimulation in biosynthesis under dynamic compression appears to be enhanced when more matrix is present. The data of Fig. 10 also show an increase in stimulation in the outer ring compared to the center when more matrix is present.

Some possible mechanisms involved in the transduction of small amplitude dynamic compression to a cellular response are: (1) altered fluid pressure; (2) enhanced fluid flow (transport); (3) induced streaming potentials; (4) cell-matrix interactions; and (5) growth factor release from matrix binding sites or by cells. Physicochemical changes are probably not significant, since the disk volume is nearly constant with compression amplitudes of ~3%. Oscillatory compression will generally increase fluid pressure more in the center than in the ring while fluid velocities will be higher in the ring than in the center due to the unconfined geometry (Kim et al., 1994, 1995). The outer ring showed greater stimulation in radiolabel incorporation than the center. Thus, it is unlikely that altered pressure is responsible for the stimulation of biosynthesis in dynamically compressed CA disks, whereas mechanisms related to fluid flow are consistent with a greater stimulation in the ring. The maximum fluid pressures induced in dynamic compression are approximately equal to the measured stress (Kim et al., 1995). For CA disks at late times, the measured stress was ≈30 kPa for a 30 μm displacement imposed on a 1 mm thick specimen. This is relatively small compared to the levels of pressure which have been observed to affect chondrocyte synthetic rates (>1 MPa) (Hall et al., 1991) and is approximately 10-20% that in calf cartilage disks. The level of stimulation of biosynthesis seen here is of the same order as that seen in cartilage disks, but with compression-induced fluid pressures about an order of magnitude lower.

The magnitude of the relative fluid velocity corresponding to the known values of frequency, displacement, and disk

thickness is proportional to the product of the modulus and the hydraulic permeability, $H_A \times k$ (Kim et al., 1995). From the data of Fig. 7, this product was calculated to be relatively constant at 0.5×10^{-9} m^2/s during the entire culture (up to 47 days). The product $H_A \times k$ for parent cartilage explants is also of the same magnitude. Therefore fluid velocities within explant and CA disks are of the same order of magnitude. Since the stimulation of synthesis by dynamic compression for both CA and explant disks is in the 10-40% range, mechanisms dependent on bulk fluid flow within the disk could play a role. For example, convective transport of mobile solutes in the extracellular fluid could be enhanced by dynamic compression. Given fluid velocities of ~1 μm/s over dimensions of ~30 μm, the Peclet number (i.e. the ratio of convective-transport/diffusive-transport for a given solute) is 3×10^{-7} cm^2 s^{-1}/D, where D is the solute diffusion coefficient. Therefore, transport of small molecules (M_r<500) with D $\geq10^{-7}$ cm^2/s will not be significantly enhanced by compression induced convection. However, transport of larger molecules may be affected. In addition to modulating transport, fluid flow can also generate shear stress at the cell surface, an important factor in the response of endothelial cells to luminal flow (Dull and Davies, 1991). Fluid flow can also redistribute and deform ECM components through viscous forces. Hence the discussion of cell-matrix interactions for static compression applies here as well. Electric fields (streaming potentials) are generated by fluid flow convecting mobile counterions past ionized charge groups on immobilized macromolecules (Grodzinsky, 1983). Streaming potential fields are proportional to both fluid velocity and matrix fixed charge density. In this context, an increase in stimulated biosynthetic response at later times in culture would be consistent with a greater fixed charge density even though bulk fluid velocities may not increase significantly with time in culture (at constant applied dynamic compression amplitude).

In summary, chondrocytes cultured in agarose synthesize, assemble and maintain an ECM containing macromolecules characteristic of the chondrocyte phenotype. The mechanical properties of these CA disks develop during culture to approach those of intact articular cartilage. We have further shown here that chondrocytes in agarose which have synthesized a cell-associated matrix exhibit a biosynthetic response to compression which is similar to that of explanted cartilage. Current evidence points towards the predominance of cell-matrix interactions, and fluid flow with its associated electric fields as important players informing the chondrocyte of its mechanical environment. Based on these findings, we believe that the flexibility of the agarose system should enable more detailed characterization of transduction pathways in the cellular response to mechanical signals. Such information will be of use in understanding normal physiology, pathologies (i.e. osteoarthritis), and development of cartilage.

This research was supported by NIH Grant AR33236, AFOSR Grant 91-0153, and the AO/ASIF-Foundation, Switzerland; MDB also received fellowship support from the Whitaker Health Sciences Fund, the Natural Sciences and Engineering Research Council of Canada and the Medical Research Council of Canada. The authors thank Drs Robert Sah, Young-Jo Kim, and Tom Quinn for many helpful discussions.

REFERENCES

Adams, J. C. and Watt, F. M. (1993). Regulation of development and differentiation by the extracellular matrix. *Development* **117**, 1183-1198.

Akeson, W. H., Woo, S. J. Y., Amiel, D., Coutts, R. D. and Daniel, D. (1973). The connective tissue response to immobility: biochemical changes in periarticular connective tissue of the immobilized rabbit knee. *Clin. Orthop.* **93**, 356-362.

Arokoski, J., Kiviranta, I., Jurvelin, J., Tammi, M. and Helminen, H. J. (1993). Long-distance running causes site-dependent decrease of cartilage glycosaminoglycan content in the knee joints of beagle dogs. *Arthritis Rheum.* **36**, 1451-1459.

Aydelotte, M. B., Schleyerbach, R., Zeck, B. J. and Kuettner, K. E. (1986). Articular chondrocytes cultured in agarose gel for study of chondrocytic chondrolysis. In *Articular Cartilage Biochemistry* (ed. K. E. Kuettner, R. Schleyerbach and V. C. Hascall), pp. 235-256. Raven Press, New York, NY.

Aydelotte, M. B., Greenhill, R. R. and Kuettner, K. E. (1988). Differences between sub-populations of cultured bovine articular chondrocytes. II. Proteoglycan metabolism. *Conn. Tissue Res.* **18**, 223-234.

Benya, P. D. and Shaffer, J. D. (1982). Dedifferentiated chondrocytes reexpress the differentiated collagen phenotype when cultured in agarose gels. *Cell* **30**, 215-224.

Boustany, N. N., Gray, M. L., Black, A. C. and Hunziker, E. B. (1995). The role of interstitial pH in regulating the biosynthetic response of chondrocytes to static mechanical loading. *J. Orthop. Res.* (in press).

Buschmann, M. D. (1992). Chondrocytes in agarose culture: development of a mechanically functional matrix, biosynthetic response to compression and molecular model of the modulus. PhD thesis, Massachusetts Institute of Technology, Cambridge, MA.

Buschmann, M. D., Gluzband, Y. A., Grodzinsky, A. J., Kimura, J. H. and Hunziker, E. B. (1992). Chondrocytes in agarose culture synthesize a mechanically functional extracellular matrix. *J. Orthop. Res.* **10**, 745-758.

Buschmann, M. D. and Grodzinsky, A. J. (1995). A molecular model of proteoglycan associated electrostatic forces in cartilage mechanics. *J. Biomech. Eng.* (in press).

Caterson, B. and Lowther, D. A. (1978). Changes in the metabolism of the proteoglycans from sheep articular cartilage in response to mechanical stress. *Biochim. Biophys. Acta* **540**, 412-422.

Dull, R. O. and Davies, P. F. (1991). Flow modulation of agonist (ATP)-response (Ca^{++}) coupling in vascular endothelial cells. *Am. J. Physiol.* **261**, H149-H154.

Durr, J., Goodman, S., Ptotcnik, A., von der Mark, H. and von der Mark, K. (1993). Localization of β1 integrins in human cartilage and their role in chondrocyte adhesion to collagen and fibronectin. *Exp. Cell Res.* **207**, 235-244.

Enomoto, M., Leboy, P. S., Menko, A. S. and Boettiger, D. (1993). β1 integrins mediate chondrocyte interaction with type I collagen, type II collagen and fibronectin. *Exp. Cell Res.* **205**, 276-285.

Farndale, R. W., Buttle, D. J. and Barrett, A. J. (1986). Improved quantitation and discrimination of sulphated glycosaminoglycans by use of dimethylmethylene blue. *Biochim. Biophys. Acta* **883**, 173-177.

Flannery, C. R. and Sandy, J. D. (1994). Chondrocyte expression of CD44, TSG-6 and RHAMM: Effect of retinoic acid, IL-1 and TNF treatment on hyaluronan receptor gene products. *Trans. Orth. Res. Soc.* **19**, 76.

Frank, E. H. and Grodzinsky, A. J. (1987). Cartilage electromechanics - II. A continuum model of cartilage electrokinetics and correlation with experiments. *J. Biomech.* **20**, 629-639.

Freeman, P. M., Natarajan, R., Kimura, J. H. and Andriacchi, T. P. (1994). Chondrocyte cells respond mechanically to compressive loads. *J. Orthop. Res.* **12**, 311-320.

Gray, M. L., Pizzanelli, A. M., Grodzinsky, A. J. and Lee, R. C. (1988). Mechanical and physicochemical determinants of the chondrocyte biosynthetic response. *J. Orthop. Res.* **6**, 777-792.

Grodzinsky, A. J. (1983). Electromechanical and physicochemical properties of connective tissue. *CRC Crit. Rev. Bioeng.* **9**, 133-199.

Hall, A. C., Urban, J. P. G. and Gehl, K. A. (1991). The effects of hydrostatic pressure on matrix synthesis in articular cartilage. *J. Orthop. Res.* **9**, 1-10.

Hardingham, T. E. and Fosang, A. J. (1992). Proteoglycans: many forms and functions. *FASEB J.* **6**, 861-870.

Hodge, W. A., Fijan, R. S., Carlson, K. L., Burgess, R. G., Harris, W. H. and Mann, R. W. (1986). Contact pressures in the human hip joint measured in vivo. *Proc. Nat. Acad. Sci. USA* **83**, 2879-2883.

Hunziker, E. B., Herrmann, W. and Schenk, R. K. (1982). Improved

cartilage fixation by ruthenium hexaammine trichloride. *J. Ultrastruct. Res.* **81**, 1-12.

Inerot, S., Heinegard, D., Olsson, S.-E., Telhag, H. and Audell, L. (1991). Proteoglycan alterations during developing experimental osteoarthritis in a novel hip joint model. *J. Orthop. Res.* **9**, 658-673.

Ingber, D. (1991). Integrins as mechanochemical transducers. *Curr. Opin. Cell Biol.* **3**, 841-848.

Jurvelin, J., Kiviranta, I., Saamanen, A.-M., Tammi, M. and Helminen, H. J. (1990). Indentation stiffness of young canine knee articular cartilage: Influence of strenuous joint loading. *J. Biomech.* **23**, 1239-1246.

Kim, Y. J., Sah, R. L. Y., Doong, J. Y. H. and Grodzinsky, A. J. (1988). Fluorometric assay of DNA in cartilage explants using Hoechst 33258. *Anal. Biochem.* **174**, 168-176.

Kim, Y.-J., Sah, R. L.-Y., Grodzinsky, A. J., Plaas, A. H. K. and Sandy, J. D. (1994). Mechanical regulation of cartilage biosynthetic behavior: physical stimuli. *Arch. Biochem. Bioph.* **311**, 1-12.

Kim, Y.-J., Bonassar, L. J. and Grodzinsky, A. J. (1995). The role of cartilage streaming potential, fluid flow and pressure in the stimulation of chondrocyte biosynthesis during dynamic compression. *J. Biomech.* (in press).

Kiviranta, I., Jurvelin, J., Tammi, M., Saamanen, A.-M. and Helminen, H. J. (1987). Weight bearing controls glycosaminoglycan concentration and articular cartilage thickness in the knee joints of young beagle dogs. *Arthritis Rheum.* **30**, 801-809.

Kiviranta, I., Tammi, M., Jurvelin, J., Saamanen, A. M. and Helminen, H. J. (1988). Moderate running exercise augments glycosaminoglycans and thickness of articular cartilage in the knee joint of young beagle dogs. *J. Orthop. Res.* **6**, 188-195.

Kiviranta, I., Tammi, M., Jurvelin, J., Arokoski, J., Saamanen, A.-M. and Helminen, H. J. (1992). Articular cartilage thickness and glycosaminoglycan distribution in the canine knee joint after strenuous (20km/day) running exercise. *Clin. Orthop.* **283**, 302-308.

Knudson, C. B. and Knudson, W. (1993). Hyaluronan binding proteins in development, tissue homeostasis and disease. *FASEB J.* **7**, 1233-1241.

Korver, T. H. J., van de Stadt, R. J., Kiljan, E., van Kampen, G. P. J. and van der Korst, J. K. (1992). Effects of loading on the synthesis of proteoglycans in different layers of anatomically intact articular cartilage in vitro. *J. Rheumatol.* **19**, 905-912.

Kuettner, K. E., Pauli, B. U., Gall, G., Memoli, V. A. and Schenk, R. K. (1982). Synthesis of cartilage matrix by mammalian cells in vitro I. Isolation, culture characteristics, and morphology. *J. Cell Biol.* **93**, 743-750.

Kuettner, K. E., Schleyerbach, R. and C, H. V. (1986). *Articular Cartilage Biochemistry*, 2nd edn. Raven Press, New York, NY.

Lee, D. A. and Bader, D. L. (1994). Alterations in chondrocyte shape in agarose in response to mechanical loading and its relation to matrix production. *Trans Orth. Res. Soc.* **19**, 103.

Mankin, H. J. and Brandt, K. D. (1984). Biochemistry and metabolism of cartilage in osteoarthritis. In *Osteoarthritis* (ed. Moskowitz, R. W., Howell, D. S., Goldberg, V. M. and Mankin, H. J.), pp. 43-79. WB Saunders, Philadelphia.

Maroudas, A. (1979). Physico-chemical properties of articular cartilage. In *Adult Articular Cartilage*, 2nd edn. (ed. M. A. R. Freeman). pp. 215-290. Pitman, Tunbridge Wells, England.

Mow, V. C., Kuei, S. C., Lai, W. M. and Armstrong, C. G. (1980). Biphasic creep and stress relaxation of articular cartilage in compression: Theory and experiments. *J. Biomech. Eng.* **102**, 73-84.

Mow, V. C., Holmes, M. H. and Lai, W. M. (1984). Fluid transport and mechanical properties of articular cartilage: A review. *J. Biomech.* **17**, 377-394.

Olah, E. H. and Kostenszky, K. S. (1972). Effect of altered functional demand on the glycosaminoglycan content of the articular cartilage of dogs. *Acta Biol. Hung.* **23**, 195-200.

Palmoski, M. J., Perricone, E. and Brandt, K. D. (1979). Development and reversal of a proteoglycan aggregation defect in normal canine knee cartilage after immobilization. *Arthritis Rheum.* **22**, 508-517.

Parkkinen, J. J., Lammi, M. J., Helminen, H. J. and Tammi, M. (1992). Local stimulation of proteoglycan synthesis in articular cartilage explants by dynamic compression in vitro. *J. Orthop. Res.* **10**, 610-620.

Sah, R. L.-Y., Kim, Y.-J., Doong, J.-Y. H., Grodzinsky, A. J., Plaas, A. H. K. and Sandy, J. D. (1989). Biosynthetic response of cartilage explants to dynamic compression. *J. Orthop. Res.* **7**, 619-636.

Salter, R. B., Simmonds, D. F., Malcolm, B. W., Rumble, E. J., MacMichael, D. and Clements, N. D. (1980). The biological effect of continuous passive motion on the healing of full-thickness defects in articular cartilage. *J. Bone Joint Surg.* **62A**, 1232-1251.

Schneiderman, R., Keret, D. and Maroudas, A. (1986). Effects of mechanical and osmotic pressure on the rate of glycosaminoglycan synthesis in the human adult femoral head cartilage: An in vitro study. *J. Orthop. Res.* **4**, 393-408.

Sun, D., Aydelotte, M. B., Maldonado, B., Kuettner, K. E. and Kimura, J. H. (1986). Clonal analysis of the population of chondrocytes from the swarm rat chondrosarcoma in agarose culture. *J. Orthop. Res.* **4**, 427-436.

Tomlinson, N. and Maroudas, A. (1980). The effect of cyclic and continuous compression on the penetration of large molecules into articular cartilage. *J. Bone Joint Surg.* **62B**, 251.

(Received 1 November 1994 - Accepted 6 January 1995)